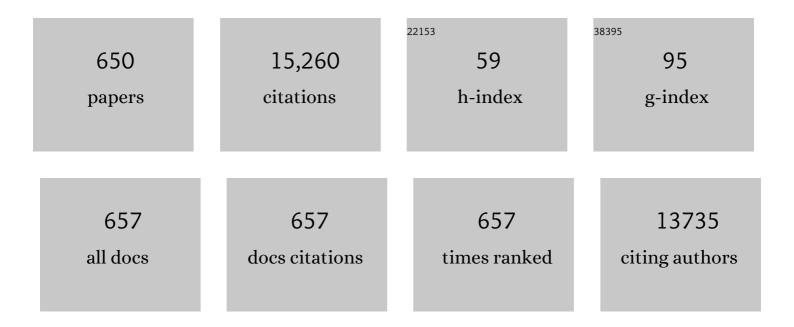
## **Gilles** Patriarche

List of Publications by Year in descending order

Source: https://exaly.com/author-pdf/4271178/publications.pdf Version: 2024-02-01



#	Article	IF	CITATIONS
1	Crystal Phase Control during Epitaxial Hybridization of Illâ€V Semiconductors with Silicon. Advanced Electronic Materials, 2022, 8, 2100777.	5.1	18
2	In‣itu Transmission Electron Microscopy Observation of Germanium Growth on Freestanding Graphene: Unfolding Mechanism of 3D Crystal Growth During Van der Waals Epitaxy. Small, 2022, 18, e2101890.	10.0	5
3	Up to 300â€K lasing with GeSn-On-Insulator microdisk resonators. Optics Express, 2022, 30, 3954.	3.4	16
4	In-plane InGaAs/Ga(As)Sb nanowire based tunnel junctions grown by selective area molecular beam epitaxy. Nanotechnology, 2022, 33, 145201.	2.6	1
5	Influence of Sapphire Substrate Orientation on the van der Waals Epitaxy of III-Nitrides on 2D Hexagonal Boron Nitride: Implication for Optoelectronic Devices. ACS Applied Nano Materials, 2022, 5, 791-800.	5.0	12
6	Nanoindentation investigation of solid-solution strengthening in III-V semiconductor alloys. International Journal of Materials Research, 2022, 96, 1237-1241.	0.3	3
7	Guided-Mode Resonator Coupled with Nanocrystal Intraband Absorption. ACS Photonics, 2022, 9, 985-993.	6.6	10
8	Electroluminescence from nanocrystals above 2 µm. Nature Photonics, 2022, 16, 38-44.	31.4	25
9	Evidence for highly p-type doping and type II band alignment in large scale monolayer WSe <sub>2</sub> /Se-terminated GaAs heterojunction grown by molecular beam epitaxy. Nanoscale, 2022, 14, 5859-5868.	5.6	12
10	Regulated Dynamics with Two Monolayer Steps in Vapor–Solid–Solid Growth of Nanowires. ACS Nano, 2022, 16, 4397-4407.	14.6	5
11	Photo-Activated Phosphorescence of Ultrafine ZnS:Mn Quantum Dots: On the Lattice Strain Contribution. Journal of Physical Chemistry C, 2022, 126, 1531-1541.	3.1	1
12	Continuous-Wave Second-Harmonic Generation in Orientation-Patterned Gallium Phosphide Waveguides at Telecom Wavelengths. ACS Photonics, 2022, 9, 2032-2039.	6.6	7
13	Indentation behaviour of (011) thin films of Ill–V semiconductors: polarity effect differences between GaAs and InP. International Journal of Materials Research, 2022, 97, 1230-1234.	0.3	0
14	Experimental quantification of atomically-resolved HAADF-STEM images using EDX. Ultramicroscopy, 2021, 220, 113152.	1.9	3
15	Engineering a Robust Flat Band in III–V Semiconductor Heterostructures. Nano Letters, 2021, 21, 680-685.	9.1	19
16	Efficient Electrical Transport Through Oxideâ€Mediated InPâ€onâ€Si Hybrid Interfaces Bonded at 300 °C. Physica Status Solidi (A) Applications and Materials Science, 2021, 218, 2000317.	1.8	1
17	Topological surface states in epitaxial <mml:math< td=""><td></td><td></td></mml:math<>		

#	Article	IF	CITATIONS
19	Development of a cryogenic indentation tool with in situ optical observation, application to the mechanical characterization of II–VI semiconductors. Semiconductor Science and Technology, 2021, 36, 035015.	2.0	2
20	Interdiffusion of Al and Ga in AlN/AlGaN superlattices grown by ammonia-assisted molecular beam epitaxy. Superlattices and Microstructures, 2021, 150, 106801.	3.1	8
21	Strain, magnetic anisotropy, and composition modulation in hybrid metal–oxide vertically assembled nanocomposites. MRS Bulletin, 2021, 46, 136-141.	3.5	5
22	Development of Micron Sized Photonic Devices Based on Deep GaN Etching. Photonics, 2021, 8, 68.	2.0	4
23	Temperature dependence of optical properties of InAs/InP quantum rod-nanowires grown on Si substrate. Journal of Luminescence, 2021, 231, 117814.	3.1	2
24	Degradation Mechanism of Porous Metal-Organic Frameworks by In Situ Atomic Force Microscopy. Nanomaterials, 2021, 11, 722.	4.1	26
25	Band-Gap Landscape Engineering in Large-Scale 2D Semiconductor van der Waals Heterostructures. ACS Nano, 2021, 15, 7279-7289.	14.6	28
26	Fabrication and characterization of ZnO:Sb/n-ZnO homojunctions. Applied Physics A: Materials Science and Processing, 2021, 127, 1.	2.3	2
27	Correlating Structure and Detection Properties in HgTe Nanocrystal Films. Nano Letters, 2021, 21, 4145-4151.	9.1	23
28	Monolithic Free-Standing Large-Area Vertical III-N Light-Emitting Diode Arrays by One-Step h-BN-Based Thermomechanical Self-Lift-Off and Transfer. ACS Applied Electronic Materials, 2021, 3, 2614-2621.	4.3	8
29	MOVPE of GaN-based mixed dimensional heterostructures on wafer-scale layered 2D hexagonal boron nitride—A key enabler of III-nitride flexible optoelectronics. APL Materials, 2021, 9, .	5.1	9
30	Spray-Drying Polymer Encapsulation of CsPbBr3 Perovskite Nanocrystals with Enhanced Photostability for LED Downconverters. ACS Applied Nano Materials, 2021, 4, 7502-7512.	5.0	11
31	Electronic band gap of van der Waals Î $\pm$ -As2Te3 crystals. Applied Physics Letters, 2021, 119, .	3.3	4
32	Selective target protein detection using a decorated nanopore into a microfluidic device. Biosensors and Bioelectronics, 2021, 183, 113195.	10.1	17
33	Dynamics of Droplet Consumption in Vapor–Liquid–Solid III–V Nanowire Growth. Crystal Growth and Design, 2021, 21, 4647-4655.	3.0	6
34	Single-Electron Tunneling PbS/InP Heterostructure Nanoplatelets for Synaptic Operations. ACS Applied Materials & Interfaces, 2021, 13, 38450-38457.	8.0	3
35	Monodispersed MOF-808 Nanocrystals Synthesized via a Scalable Room-Temperature Approach for Efficient Heterogeneous Peptide Bond Hydrolysis. Chemistry of Materials, 2021, 33, 7057-7066.	6.7	51
36	Relaxation mechanism of GaP grown on 001 Si substrates: influence of defects on the growth of AlGaP layers on GaP/Si templates. Philosophical Magazine, 2021, 101, 2189-2199.	1.6	1

#	Article	IF	CITATIONS
37	Quantum well interband semiconductor lasers highly tolerant to dislocations. Optica, 2021, 8, 1397.	9.3	14
38	Highly linear polarized emission at telecom bands in InAs/InP quantum dot-nanowires by geometry tailoring. Nanoscale, 2021, 13, 16952-16958.	5.6	1
39	Porous nanoparticles with engineered shells release their drug cargo in cancer cells. International Journal of Pharmaceutics, 2021, 610, 121230.	5.2	7
40	Comparative Study on the Quality of Microcrystalline and Epitaxial Silicon Films Produced by PECVD Using Identical SiF4 Based Process Conditions. Materials, 2021, 14, 6947.	2.9	2
41	GeSnOI mid-infrared laser technology. Light: Science and Applications, 2021, 10, 232.	16.6	18
42	Effects of nitrogen incorporation and thermal annealing on the optical and spin properties of GaPN dilute nitride alloys. Journal of Alloys and Compounds, 2020, 814, 152233.	5.5	3
43	Molecular-beam epitaxy of GaSb on 6°-offcut (0â€ <sup>−</sup> 0â€ <sup>−</sup> 1) Si using a GaAs nucleation layer. Journal of Crystal Growth, 2020, 529, 125299.	1.5	6
44	Gate length dependent transport properties of in-plane core-shell nanowires with raised contacts. Nano Research, 2020, 13, 61-66.	10.4	1
45	Nanoscale electrical analyses of axial-junction GaAsP nanowires for solar cell applications. Nanotechnology, 2020, 31, 145708.	2.6	14
46	Microstructure of GaAs thin films grown on glass using Ge seed layers fabricated by aluminium induced crystallization. Thin Solid Films, 2020, 694, 137737.	1.8	3
47	Control of the Mechanical Adhesion of Ill–V Materials Grown on Layered h-BN. ACS Applied Materials & Interfaces, 2020, 12, 55460-55466.	8.0	14
48	Reduced Lasing Thresholds in GeSn Microdisk Cavities with Defect Management of the Optically Active Region. ACS Photonics, 2020, 7, 2713-2722.	6.6	42
49	Highly Ordered Boron Nitride/Epigraphene Epitaxial Films on Silicon Carbide by Lateral Epitaxial Deposition. ACS Nano, 2020, 14, 12962-12971.	14.6	14
50	Stable and high yield growth of GaP and In <sub>0.2</sub> Ga <sub>0.8</sub> As nanowire arrays using In as a catalyst. Nanoscale, 2020, 12, 18240-18248.	5.6	6
51	Effectiveness of selective area growth using van der Waals h-BN layer for crack-free transfer of large-size III-N devices onto arbitrary substrates. Scientific Reports, 2020, 10, 21709.	3.3	12
52	Effect of sintering germanium epilayers on dislocation dynamics: From theory to experimental observation. Acta Materialia, 2020, 200, 608-618.	7.9	2
53	Why is it difficult to grow spontaneous ZnO nanowires using molecular beam epitaxy?. Nanotechnology, 2020, 31, 385601.	2.6	4
54	Crystal phase engineering of self-catalyzed GaAs nanowires using a RHEED diagram. Nanoscale Advances, 2020, 2, 2127-2134.	4.6	11

#	Article	IF	CITATIONS
55	Measuring the surface bonding energy: A comparison between the classical double-cantilever beam experiment and its nanoscale analog. AIP Advances, 2020, 10, 045006.	1.3	1
56	Ultra-low-threshold continuous-wave and pulsed lasing in tensile-strained GeSn alloys. Nature Photonics, 2020, 14, 375-382.	31.4	145
57	Encapsulation of Microperoxidase-8 in MIL-101(Cr)-X Nanoparticles: Influence of Metal–Organic Framework Functionalization on Enzymatic Immobilization and Catalytic Activity. ACS Applied Nano Materials, 2020, 3, 3233-3243.	5.0	26
58	Phase Selection in Self-catalyzed GaAs Nanowires. Nano Letters, 2020, 20, 1669-1675.	9.1	83
59	Pushing Absorption of Perovskite Nanocrystals into the Infrared. Nano Letters, 2020, 20, 3999-4006.	9.1	18
60	Efficient incorporation and protection of lansoprazole in cyclodextrin metal-organic frameworks. International Journal of Pharmaceutics, 2020, 585, 119442.	5.2	15
61	Single crystalline boron rich B(Al)N alloys grown by MOVPE. Applied Physics Letters, 2020, 116, .	3.3	12
62	Engineering dislocations and nanovoids for high-efficiency III–V photovoltaic cells on silicon. AIP Conference Proceedings, 2020, , .	0.4	2
63	Density-controlled growth of vertical InP nanowires on Si(111) substrates. Nanotechnology, 2020, 31, 354003.	2.6	4
64	Zinc-blende group III-V/group IV epitaxy: Importance of the miscut. Physical Review Materials, 2020, 4, .	2.4	23
65	Structural, vibrational, and magnetic properties of self-assembled CoPt nanoalloys embedded in SrTiO3. Physical Review Materials, 2020, 4, .	2.4	2
66	(Invited) Tensile Strain Engineering and Defects Management in GeSn Laser Cavities. ECS Transactions, 2020, 98, 61-68.	0.5	1
67	3.3 Âμm interband-cascade resonant-cavity light-emitting diode with narrow spectral emission linewidth. Semiconductor Science and Technology, 2020, 35, 125029.	2.0	6
68	Defects management in the gain media of GeSn micro-disk lasers. , 2020, , .		0
69	Capturing the Effects of Free Surfaces on Threading Dislocation Density Reduction. ECS Transactions, 2020, 98, 527-532.	0.5	1
70	Composition and Face Polarity Influences on Mechanical Properties of (111) Cd1â^'yZnyTe Determined by Indentation. Journal of Electronic Materials, 2019, 48, 6985-6990.	2.2	1
71	Evidence for a narrow band gap phase in 1T′ WS2 nanosheet. Applied Physics Letters, 2019, 115, .	3.3	25
72	Voided Ge/Si Platform to Integrate III-V Materials on Si. ECS Transactions, 2019, 93, 81-85.	0.5	3

#	Article	IF	CITATIONS
73	Ultra-Low Threshold CW Lasing in Tensile Strained GeSn Microdisk Cavities. , 2019, , .		0
74	Uprooting defects to enable high-performance Ill–V optoelectronic devices on silicon. Nature Communications, 2019, 10, 4322.	12.8	44
75	Physical mechanisms involved in the formation and operation of memory devices based on a monolayer of gold nanoparticle-polythiophene hybrid materials. Nanoscale Advances, 2019, 1, 2718-2726.	4.6	8
76	Largeâ€Area van der Waals Epitaxial Growth of Vertical IIIâ€Nitride Nanodevice Structures on Layered Boron Nitride. Advanced Materials Interfaces, 2019, 6, 1900207.	3.7	12
77	GaAs (1 1 1) epilayers grown by MBE on Ge (1 1 1): Twin reduction and polarity. Journal of Crystal Growth, 2019, 519, 84-90.	1.5	13
78	Importance of point defect reactions for the atomic-scale roughness of Ill–V nanowire sidewalls. Nanotechnology, 2019, 30, 324002.	2.6	5
79	Evidence and control of unintentional As-rich shells in GaAs <sub>1–<i>x</i> </sub> P <i> <sub>x</sub> </i> nanowires. Nanotechnology, 2019, 30, 294003.	2.6	4
80	Controlled Dislocations Injection in N/P Hg1â^'xCdxTe Photodiodes by Indentations. Journal of Electronic Materials, 2019, 48, 6108-6112.	2.2	2
81	Correlated optical and structural analyses of individual GaAsP/GaP core–shell nanowires. Nanotechnology, 2019, 30, 304001.	2.6	7
82	Trap-Free Heterostructure of PbS Nanoplatelets on InP(001) by Chemical Epitaxy. ACS Nano, 2019, 13, 1961-1967.	14.6	7
83	Selective area molecular beam epitaxy of InSb nanostructures on mismatched substrates. Journal of Crystal Growth, 2019, 512, 6-10.	1.5	13
84	InAs quantum dot in a needlelike tapered InP nanowire: a telecom band single photon source monolithically grown on silicon. Nanoscale, 2019, 11, 21847-21855.	5.6	19
85	Wafer-scale MOVPE growth and characterization of highly ordered h-BN on patterned sapphire substrates. Journal of Crystal Growth, 2019, 509, 40-43.	1.5	11
86	InAs/GaSb thin layers directly grown on nominal (0â€ <sup>−</sup> 0â€ <sup>−</sup> 1)-Si substrate by MOVPE for the fabrication of InAs FINFET. Journal of Crystal Growth, 2019, 510, 18-22.	1.5	3
87	Development of reflective back contacts for high-efficiency ultrathin Cu(In,Ga)Se2 solar cells. Thin Solid Films, 2019, 672, 1-6.	1.8	22
88	MOVPE van der Waals epitaxial growth of AlGaN/AlGaN multiple quantum well structures with deep UV emission on large scale 2D h-BN buffered sapphire substrates. Journal of Crystal Growth, 2019, 507, 352-356.	1.5	8
89	Growth optimization and characterization of regular arrays of GaAs/AlGaAs core/shell nanowires for tandem solar cells on silicon. Nanotechnology, 2019, 30, 084005.	2.6	16
90	Phase separation and surface segregation in Co–Au–SrTiO3 thin films: Self-assembly of bilayered epitaxial nanocolumnar composites. Physical Review Materials, 2019, 3, .	2.4	4

#	Article	IF	CITATIONS
91	A study of the strain distribution by scanning X-ray diffraction on GaP/Si for III–V monolithic integration on silicon. Journal of Applied Crystallography, 2019, 52, 809-815.	4.5	2
92	A porous Ge/Si interface layer for defect-free III-V multi-junction solar cells on silicon. , 2019, , .		5
93	Heteroepitaxial growth of silicon on GaAs via low-temperature plasma-enhanced chemical vapor deposition. , 2019, , .		2
94	Polarization- and diffraction-controlled second-harmonic generation from semiconductor metasurfaces. Journal of the Optical Society of America B: Optical Physics, 2019, 36, E55.	2.1	20
95	High structural and optical quality of III-V-on-Si 1.2 nm-thick oxide-bonded hybrid interface. Microelectronic Engineering, 2018, 192, 25-29.	2.4	1
96	Determination of the spin orbit coupling and crystal field splitting in wurtzite InP by polarization resolved photoluminescence. Applied Physics Letters, 2018, 112, .	3.3	4
97	Measuring and Modeling the Growth Dynamics of Self-Catalyzed GaP Nanowire Arrays. Nano Letters, 2018, 18, 701-708.	9.1	55
98	Shear-driven phase transformation in silicon nanowires. Nanotechnology, 2018, 29, 125601.	2.6	28
99	Biomimetic ion channels formation by emulsion based on chemically modified cyclodextrin nanotubes. Faraday Discussions, 2018, 210, 41-54.	3.2	8
100	Quantum cascade lasers grown on silicon. , 2018, , .		0
101	Interface energy analysis of Ill–V islands on Si (001) in the Volmer-Weber growth mode. Applied Physics Letters, 2018, 113, .	3.3	14
102	Nanoscale investigation of a radial p–n junction in self-catalyzed GaAs nanowires grown on Si (111). Nanoscale, 2018, 10, 20207-20217.	5.6	10
103	Solid-State Nanopore Easy Chip Integration in a Cheap and Reusable Microfluidic Device for Ion Transport and Polymer Conformation Sensing. ACS Sensors, 2018, 3, 2129-2137.	7.8	21
104	Atomic Step Flow on a Nanofacet. Physical Review Letters, 2018, 121, 166101.	7.8	113
105	A Stressâ€Free and Textured GaP Template on Silicon for Solar Water Splitting. Advanced Functional Materials, 2018, 28, 1801585.	14.9	22
106	Wave-Function Engineering in HgSe/HgTe Colloidal Heterostructures To Enhance Mid-infrared Photoconductive Properties. Nano Letters, 2018, 18, 4590-4597.	9.1	24
107	Coupled HgSe Colloidal Quantum Wells through a Tunable Barrier: A Strategy To Uncouple Optical and Transport Band Gap. Chemistry of Materials, 2018, 30, 4065-4072.	6.7	32
108	In-plane InSb nanowires grown by selective area molecular beam epitaxy on semi-insulating substrate. Nanotechnology, 2018, 29, 305705.	2.6	20

#	Article	IF	CITATIONS
109	Versatile cyclodextrin nanotube synthesis with functional anchors for efficient ion channel formation: design, characterization and ion conductance. Nanoscale, 2018, 10, 15303-15316.	5.6	11
110	Impact of the sequence of precursor introduction on the growth and properties of atomic layer deposited Al-doped ZnO films. Journal of Vacuum Science and Technology A: Vacuum, Surfaces and Films, 2018, 36, .	2.1	11
111	Quantum cascade lasers grown on silicon. Scientific Reports, 2018, 8, 7206.	3.3	56
112	Universal description of III-V/Si epitaxial growth processes. Physical Review Materials, 2018, 2, .	2.4	43
113	Chemical nature of the anion antisite in dilute phosphide <mml:math xmlns:mml="http://www.w3.org/1998/Math/MathML"&gt;<mml:mrow><mml:mi>GaA</mml:mi><mml:msub><mml mathvariant="normal"&gt;s<mml:mrow><mml:mn>1</mml:mn><mml:mo>â^^</mml:mo><mml:mi>xmathvariant="normal"&gt;P</mml:mi><mml:mi>x</mml:mi></mml:mrow></mml </mml:msub></mml:mrow> alloy</mml:math 	:mi ml2mai> <td>nm<b>l</b>:mrow&gt;<!--</td--></td>	nm <b>l</b> :mrow> </td
114	Ultrathin Ni nanowires embedded in <mml:math .<br="" 2,="" 2010,="" trals,="">xmlns:mml="http://www.w3.org/1998/Math/MathML"&gt;<mml:msub><mml:mi>SrTiO</mml:mi><mml:mn>3: Vertical epitaxy, strain relaxation mechanisms, and solid-state amorphization. Physical Review Materials, 2018, 2, .</mml:mn></mml:msub></mml:math>	ıl:mn> 2.4	ml:msub>
115	Atomic scale analyses of {b Z}-module defects in an NiZr alloy. Acta Crystallographica Section A: Foundations and Advances, 2018, 74, 647-658.	0.1	2
116	Large angle twist-bonded compliant substrates for the epitaxy of lattice mismatched III-V semiconductors. , 2018, , 193-196.		0
117	Z-modules in crystallography: structures and defects. Acta Crystallographica Section A: Foundations and Advances, 2018, 74, e103-e104.	0.1	0
118	Threading dislocation free GaSb nanotemplates grown by selective molecular beam epitaxy on GaAs (001) for in-plane InAs nanowire integration. Journal of Crystal Growth, 2017, 477, 45-49.	1.5	13
119	Nanoselective area growth of defect-free thick indium-rich InGaN nanostructures on sacrificial ZnO templates. Nanotechnology, 2017, 28, 195304.	2.6	1
120	Characterization of antimonide based material grown by molecular epitaxy on vicinal silicon substrates via a low temperature AlSb nucleation layer. Journal of Crystal Growth, 2017, 477, 65-71.	1.5	15
121	Flexible metal-semiconductor-metal device prototype on wafer-scale thick boron nitride layers grown by MOVPE. Scientific Reports, 2017, 7, 786.	3.3	41
122	Morphology and valence band offset of GaSb quantum dots grown on GaP(001) and their evolution upon capping. Nanotechnology, 2017, 28, 225601.	2.6	8
123	Dynamic Characterization of III-Nitride-Based High-Speed Photodiodes. IEEE Photonics Journal, 2017, 9, 1-7.	2.0	20
124	In Situ Optical Monitoring of New Pathways in the Metal-Induced Crystallization of Amorphous Ge. Crystal Growth and Design, 2017, 17, 5783-5789.	3.0	7
125	<i>In situ</i> passivation of GaAsP nanowires. Nanotechnology, 2017, 28, 495707.	2.6	27
126	Electronic properties of (Sb;Bi)2Te3 colloidal heterostructured nanoplates down to the single particle level. Scientific Reports, 2017, 7, 9647.	3.3	7

#	Article	IF	CITATIONS
127	Emission wavelength red-shift by using "semi-bulk―InGaN buffer layer in InGaN/InGaN multiple-quantum-well. Superlattices and Microstructures, 2017, 112, 279-286.	3.1	7
128	Surface effects on exciton diffusion in non polar ZnO/ZnMgO heterostructures. Journal of Physics Condensed Matter, 2017, 29, 485706.	1.8	2
129	Functionalized Solid-State Nanopore Integrated in a Reusable Microfluidic Device for a Better Stability and Nanoparticle Detection. ACS Applied Materials & Interfaces, 2017, 9, 41634-41640.	8.0	42
130	Gas sensors boosted by two-dimensional h-BN enabled transfer on thin substrate foils: towards wearable and portable applications. Scientific Reports, 2017, 7, 15212.	3.3	54
131	Enhanced sputtering of Ge nanowires under synergetic effect of Mn ion and electron beams. Results in Physics, 2017, 7, 3813-3814.	4.1	0
132	Study of the nucleation and growth of InP nanowires on silicon with gold-indium catalyst. Journal of Crystal Growth, 2017, 458, 96-102.	1.5	7
133	Improving InGaN heterojunction solar cells efficiency using a semibulk absorber. Solar Energy Materials and Solar Cells, 2017, 159, 405-411.	6.2	23
134	Mask effect in nano-selective- area-growth by MOCVD on thickness enhancement, indium incorporation, and emission of InGaN nanostructures on AlN-buffered Si(111) substrates. Optical Materials Express, 2017, 7, 376.	3.0	4
135	Low-loss orientation-patterned GaSb waveguides for mid-infrared parametric conversion. Optical Materials Express, 2017, 7, 3011.	3.0	14
136	III-V Nanowires on Silicon: a possible route to Si-based tandem solar cells. , 2017, , .		0
137	Ultrathin PECVD epitaxial Si solar cells on glass via low-temperature transfer process. Progress in Photovoltaics: Research and Applications, 2016, 24, 1075-1084.	8.1	32
138	Wetâ€Route Synthesis and Characterization of Yb:CaF <sub>2</sub> Optical Ceramics. Journal of the American Ceramic Society, 2016, 99, 1992-2000.	3.8	39
139	Synthesis of In0.1Ga0.9N/GaN structures grown by MOCVD and MBE for high speed optoelectronics. MRS Advances, 2016, 1, 1735-1742.	0.9	7
140	Selective area heteroepitaxy of GaSb on GaAs (001) for in-plane InAs nanowire achievement. Nanotechnology, 2016, 27, 505301.	2.6	31
141	Nanoparticle Electrical Analysis and Detection with a Solid-state Nanopore in a Microfluidic Device. Procedia Engineering, 2016, 168, 1475-1478.	1.2	3
142	Probing the electronic properties of CVD graphene superlattices. , 2016, , .		1
143	Nanoselective area growth of GaN by metalorganic vapor phase epitaxy on 4H-SiC using epitaxial graphene as a mask. Applied Physics Letters, 2016, 108, .	3.3	15
144	New insights into the Mo/Cu(In,Ga)Se2 interface in thin film solar cells: Formation and properties of the MoSe2 interfacial layer. Journal of Chemical Physics, 2016, 145, 154702.	3.0	28

#	Article	IF	CITATIONS
145	Role of V-pits in the performance improvement of InGaN solar cells. Applied Physics Letters, 2016, 109, .	3.3	8
146	Low temperature plasma enhanced CVD epitaxial growth of silicon on GaAs: a new paradigm for III-V/Si integration. Scientific Reports, 2016, 6, 25674.	3.3	28
147	High reflectance dielectric distributed Bragg reflectors for near ultra-violet planar microcavities: SiO2/HfO2 versus SiO2/SiNx. Journal of Applied Physics, 2016, 120, .	2.5	6
148	Local probing of the interfacial strength in InP/Si substructures. MRS Advances, 2016, 1, 779-784.	0.9	0
149	Single-crystal nanopyramidal BGaN by nanoselective area growth on AlN/Si(111) and GaN templates. Nanotechnology, 2016, 27, 115602.	2.6	4
150	Pressure-Dependent Photoluminescence Study of Wurtzite InP Nanowires. Nano Letters, 2016, 16, 2926-2930.	9.1	21
151	Large-Area Two-Dimensional Layered Hexagonal Boron Nitride Grown on Sapphire by Metalorganic Vapor Phase Epitaxy. Crystal Growth and Design, 2016, 16, 3409-3415.	3.0	106
152	First orientation-patterned GaSb ridge waveguides fabrication and preliminary characterization for frequency conversion in the mid-infrared. Proceedings of SPIE, 2016, , .	0.8	1
153	(Invited) Locally Measuring the Adhesion of InP Membranes Directly Bonded on Silicon. ECS Transactions, 2016, 75, 169-176.	0.5	Ο
154	van der Waals Epitaxy of GaSe/Graphene Heterostructure: Electronic and Interfacial Properties. ACS Nano, 2016, 10, 9679-9686.	14.6	154
155	Lazarevicite-type short-range ordering in ternary III-V nanowires. Physical Review B, 2016, 94, .	3.2	7
156	Selective CO <sub>2</sub> methanation on Ru/TiO <sub>2</sub> catalysts: unravelling the decisive role of the TiO <sub>2</sub> support crystal structure. Catalysis Science and Technology, 2016, 6, 8117-8128.	4.1	84
157	Publisher's Note: Interplay between tightly focused excitation and ballistic propagation of polariton condensates in a ZnO microcavity [Phys. Rev. B92, 235308 (2015)]. Physical Review B, 2016, 93, .	3.2	0
158	Mechanistic Insight and Optimization of InP Nanocrystals Synthesized with Aminophosphines. Chemistry of Materials, 2016, 28, 5925-5934.	6.7	93
159	Band Alignment and Minigaps in Monolayer MoS <sub>2</sub> -Graphene van der Waals Heterostructures. Nano Letters, 2016, 16, 4054-4061.	9.1	288
160	Sub-nanometrically resolved chemical mappings of quantum-cascade laser active regions. Semiconductor Science and Technology, 2016, 31, 055017.	2.0	6
161	Metallic Functionalization of CdSe 2D Nanoplatelets and Its Impact on Electronic Transport. Journal of Physical Chemistry C, 2016, 120, 12351-12361.	3.1	29
162	Nondestructive Characterization of Residual Threading Dislocation Density in HgCdTe Layers Grown on CdZnTe by Liquid-Phase Epitaxy. Journal of Electronic Materials, 2016, 45, 4518-4523.	2.2	4

#	Article	IF	CITATIONS
163	An ultra-thin SiO2 ALD layer for void-free bonding of Ill–V material on silicon. Microelectronic Engineering, 2016, 162, 40-44.	2.4	6
164	Infrared Photodetection Based on Colloidal Quantum-Dot Films with High Mobility and Optical Absorption up to THz. Nano Letters, 2016, 16, 1282-1286.	9.1	150
165	Locally measuring the adhesion of InP directly bonded on sub-100 nm patterned Si. Nanotechnology, 2016, 27, 115707.	2.6	3
166	Sharpening the Interfaces of Axial Heterostructures in Self-Catalyzed AlGaAs Nanowires: Experiment and Theory. Nano Letters, 2016, 16, 1917-1924.	9.1	60
167	Chemical lift-off and direct wafer bonding of GaN/InGaN P–l–N structures grown on ZnO. Journal of Crystal Growth, 2016, 435, 105-109.	1.5	3
168	Effect of Dot-Height Truncation on the Device Performance of Multilayer InAs/GaAs Quantum Dot Solar Cells. IEEE Journal of Photovoltaics, 2016, 6, 584-589.	2.5	3
169	Photon Cascade from a Single Crystal Phase Nanowire Quantum Dot. Nano Letters, 2016, 16, 1081-1085.	9.1	37
170	Interplay between tightly focused excitation and ballistic propagation of polariton condensates in a ZnO microcavity. Physical Review B, 2015, 92, .	3.2	6
171	Nondestructive three-dimensional imaging of crystal strain and rotations in an extended bonded semiconductor heterostructure. Physical Review B, 2015, 92, .	3.2	20
172	Atomically Sharp Interface in an h-BN-epitaxial graphene van der Waals Heterostructure. Scientific Reports, 2015, 5, 16465.	3.3	62
173	Strain in a silicon-on-insulator nanostructure revealed by 3D x-ray Bragg ptychography. Scientific Reports, 2015, 5, 9827.	3.3	52
174	Nanoselective area growth and characterization of dislocation-free InGaN nanopyramids on AlN buffered Si(111) templates. Applied Physics Letters, 2015, 107, .	3.3	15
175	Type I band alignment in GaAs81Sb19/GaAs core-shell nanowires. Applied Physics Letters, 2015, 107, .	3.3	14
176	Investigation of new approaches for InGaN growth with high indium content for CPV application. AIP Conference Proceedings, 2015, , .	0.4	0
177	Abrupt GaP/Si hetero-interface using bistepped Si buffer. Applied Physics Letters, 2015, 107, .	3.3	19
178	High quality thick InGaN nanostructures grown by nanoselective area growth for new generation photovoltaic devices. Physica Status Solidi (A) Applications and Materials Science, 2015, 212, 740-744.	1.8	7
179	BAIN thin layers for deep UV applications. Physica Status Solidi (A) Applications and Materials Science, 2015, 212, 745-750.	1.8	31
180	Optical polarization properties of InAs/InP quantum dot and quantum rod nanowires. Nanotechnology, 2015, 26, 395701.	2.6	14

#	Article	IF	CITATIONS
181	Towards InAs/InGaAs/GaAs Quantum Dot Solar Cells Directly Grown on Si Substrate. Materials, 2015, 8, 4544-4552.	2.9	12
182	Oxide-Free Bonding of III-V-Based Material on Silicon and Nano-Structuration of the Hybrid Waveguide for Advanced Optical Functions. Photonics, 2015, 2, 1054-1064.	2.0	5
183	Gradient CdSe/CdS Quantum Dots with Room Temperature Biexciton Unity Quantum Yield. Nano Letters, 2015, 15, 3953-3958.	9.1	143
184	GaSb-based composite quantum wells for laser diodes operating in the telecom wavelength range near 1.55- <i><math>\hat{l}_{4}</math></i> m. Applied Physics Letters, 2015, 106, .	3.3	12
185	Interface Intermixing in Type II InAs/GalnAsSb Quantum Wells Designed for Active Regions of Mid-Infrared-Emitting Interband Cascade Lasers. Nanoscale Research Letters, 2015, 10, 471.	5.7	9
186	Silicon surface preparation for III-V molecular beam epitaxy. Journal of Crystal Growth, 2015, 413, 17-24.	1.5	27
187	Microstructural and electrical investigation of Pd/Au ohmic contact on p-GaN. Journal of Vacuum Science and Technology B:Nanotechnology and Microelectronics, 2015, 33, 010603.	1.2	15
188	Simultaneous growth of GaN/AlGaN quantum wells on c-, a-, m-, and (20.1)-plane GaN bulk substrates obtained by the ammonothermal method: Structural studies. Journal of Crystal Growth, 2015, 414, 87-93.	1.5	2
189	Role of compositional fluctuations and their suppression on the strain and luminescence of InGaN alloys. Journal of Applied Physics, 2015, 117, 055705.	2.5	20
190	Crystal growth of bullet-shaped magnetite in magnetotactic bacteria of the <i>Nitrospirae</i> phylum. Journal of the Royal Society Interface, 2015, 12, 20141288.	3.4	48
191	Abrupt GaP/GaAs Interfaces in Self-Catalyzed Nanowires. Nano Letters, 2015, 15, 6036-6041.	9.1	47
192	Quantitative evaluation of microtwins and antiphase defects in GaP/Si nanolayers for a III–V photonics platform on silicon using a laboratory X-ray diffraction setup. Journal of Applied Crystallography, 2015, 48, 702-710.	4.5	16
193	Evidence for Flat Bands near the Fermi Level in Epitaxial Rhombohedral Multilayer Graphene. ACS Nano, 2015, 9, 5432-5439.	14.6	92
194	Nanoscale elemental quantification in heterostructured SiGe nanowires. Nanoscale, 2015, 7, 8544-8553.	5.6	7
195	Crystallization of Si Templates of Controlled Shape, Size, and Orientation: Toward Micro- and Nanosubstrates. Crystal Growth and Design, 2015, 15, 2102-2109.	3.0	5
196	AlGaN-based MQWs grown on a thick relaxed AlGaN buffer on AlN templates emitting at 285 nm. Optical Materials Express, 2015, 5, 380.	3.0	30
197	Structural and optical investigations of AlGaN MQWs grown on a relaxed AlGaN buffer on AlN templates for emission at 280nm. Journal of Crystal Growth, 2015, 432, 37-44.	1.5	6
198	Biomimetic Nanotubes Based on Cyclodextrins for Ion-Channel Applications. Nano Letters, 2015, 15, 7748-7754.	9.1	30

#	Article	IF	CITATIONS
199	Nonstoichiometric Low-Temperature Grown GaAs Nanowires. Nano Letters, 2015, 15, 6440-6445.	9.1	9
200	Nanostructure and luminescence properties of amorphous and crystalline ytterbium–yttrium oxide thin films obtained with pulsed reactive crossed-beam deposition. Journal of Materials Science, 2015, 50, 1267-1276.	3.7	2
201	ZnS anisotropic nanocrystals using a one-pot low temperature synthesis. New Journal of Chemistry, 2015, 39, 90-93.	2.8	8
202	Bonding mechanism of a yttrium iron garnet film on Si without the use of an intermediate layer. Applied Physics Letters, 2014, 105, 141601.	3.3	3
203	Aberration corrected STEM to study an ancient hair dyeing formula. AIP Conference Proceedings, 2014, , ,	0.4	2
204	Void-free direct bonding of InP to Si: Advantages of low H-content and ozone activation. Journal of Vacuum Science and Technology B:Nanotechnology and Microelectronics, 2014, 32, 021201.	1.2	8
205	Nanoscale selective area growth of thick, dense, uniform, In-rich, InGaN nanostructure arrays on GaN/sapphire template. Journal of Applied Physics, 2014, 116, .	2.5	18
206	Piezoelectric effect in InAs/InP quantum rod nanowires grown on silicon substrate. Applied Physics Letters, 2014, 104, 183101.	3.3	7
207	Random stacking sequences in III-V nanowires are correlated. Physical Review B, 2014, 89, .	3.2	13
208	Interfacial abruptness in axial Si/SiGe heterostructures in nanowires probed by scanning capacitance microscopy. Physica Status Solidi (A) Applications and Materials Science, 2014, 211, 509-513.	1.8	6
209	Control of heterointerface and strain mapping in Au catalyzed axial Si-Si1-xGex nanowires. Materials Research Society Symposia Proceedings, 2014, 1707, 37.	0.1	0
210	Wafer bonding of Si for hybrid photonic devices. Materials Research Society Symposia Proceedings, 2014, 1748, 1.	0.1	0
211	Multifunctional hybrid silica nanoparticles based on [Mo6Br14]2â^' phosphorescent nanosized clusters, magnetic γ-Fe2O3 and plasmonic gold nanoparticles. Journal of Colloid and Interface Science, 2014, 424, 132-140.	9.4	24
212	Recent advances in development of vertical-cavity based short pulse source at 1.55 μm. Frontiers of Optoelectronics, 2014, 7, 1-19.	3.7	1
213	Control of the interfacial abruptness of Au-catalyzed Si-Si1â^'xGex heterostructured nanowires grown by vapor–liquid–solid. Journal of Vacuum Science and Technology A: Vacuum, Surfaces and Films, 2014, 32, .	2.1	4
214	Electrolyte-Gated Field Effect Transistor to Probe the Surface Defects and Morphology in Films of Thick CdSe Colloidal Nanoplatelets. ACS Nano, 2014, 8, 3813-3820.	14.6	61
215	Efficient Exciton Concentrators Built from Colloidal Core/Crown CdSe/CdS Semiconductor Nanoplatelets. Nano Letters, 2014, 14, 207-213.	9.1	224
216	Type-II CdSe/CdTe Core/Crown Semiconductor Nanoplatelets. Journal of the American Chemical Society, 2014, 136, 16430-16438.	13.7	153

#	Article	IF	CITATIONS
217	Highly crystalline urchin-like structures made of ultra-thin zinc oxide nanowires. RSC Advances, 2014, 4, 47234-47239.	3.6	32
218	Direct bonding of YIG film on Si without intermediate layer. , 2014, , .		0
219	Electrical transport across the heterointerface of InP membranes bonded oxide-free on Si. , 2014, , .		0
220	Incorporation and redistribution of impurities into silicon nanowires during metal-particle-assisted growth. Nature Communications, 2014, 5, 4134.	12.8	91
221	Catalyst faceting during graphene layer crystallization in the course of carbon nanofiber growth. Carbon, 2014, 79, 93-102.	10.3	5
222	Dual light-emitting nanoparticles: second harmonic generation combined with rare-earth photoluminescence. Journal of Materials Chemistry C, 2014, 2, 7681-7686.	5.5	13
223	Composition-Dependent Interfacial Abruptness in Au-Catalyzed Si <sub>1–<i>x</i></sub> Ge <sub><i>x</i></sub> /Si/Si <sub>1–<i>x</i></sub> Ge <sub><i>x</i></sub> Nanowire Heterostructures. Nano Letters, 2014, 14, 5140-5147.	9.1	34
224	Carbon Nanotube Translocation to Distant Organs after Pulmonary Exposure: Insights fromin Situ14C-Radiolabeling and Tissue Radioimaging. ACS Nano, 2014, 8, 5715-5724.	14.6	81
225	Novel Heterostructured Ge Nanowires Based on Polytype Transformation. Nano Letters, 2014, 14, 4828-4836.	9.1	61
226	Photoluminescence polarization and piezoelectric properties of InAs/InP quantum rod-nanowires. , 2014, , .		0
227	Synthesis of Zinc and Lead Chalcogenide Core and Core/Shell Nanoplatelets Using Sequential Cation Exchange Reactions. Chemistry of Materials, 2014, 26, 3002-3008.	6.7	83
228	Single step fabrication of N-doped graphene/Si3N4/SiC heterostructures. Nano Research, 2014, 7, 835-843.	10.4	17
229	Siliconâ€Microtube Scaffold Decorated with Anatase TiO <sub>2</sub> as a Negative Electrode for a 3D Litiumâ€lon Microbattery. Advanced Energy Materials, 2014, 4, 1301612.	19.5	67
230	FIB patterning of dielectric, metallized and graphene membranes: A comparative study. Microelectronic Engineering, 2014, 121, 87-91.	2.4	25
231	Investigation on Mn doping of Ge nanowires for spintronics. Physica Status Solidi C: Current Topics in Solid State Physics, 2014, 11, 315-319.	0.8	2
232	Multicharacterization approach for studying InAl(Ga)N/Al(Ga)N/GaN heterostructures for high electron mobility transistors. AIP Advances, 2014, 4, .	1.3	15
233	Instrumented nanoindentation and scanning electron transmission microscopy applied to the study of the adhesion of InP membranes heteroepitaxially bonded to Si. EPJ Applied Physics, 2014, 65, 20702.	0.7	2
234	High performance TiN gate contact on AlGaN/GaN transistor using a mechanically strain induced P-doping. Applied Physics Letters, 2014, 104, .	3.3	13

#	Article	IF	CITATIONS
235	Nanoscale Surface and Sub-Surface Chemical Analysis of SiGe Nanowires. Microscopy and Microanalysis, 2014, 20, 2052-2053.	0.4	1
236	Characteristics of HgS nanoparticles formed in hair by a chemical reaction. Philosophical Magazine, 2013, 93, 137-151.	1.6	5
237	Quantum efficiency of InAs/InP nanowire heterostructures grown on silicon substrates. Physica Status Solidi - Rapid Research Letters, 2013, 7, 878-881.	2.4	Ο
238	Resonant TE Transmission Through a Continuous Metal Film: Perspectives for Low-Loss Plasmonic Elements. Plasmonics, 2013, 8, 829-833.	3.4	3
239	Structural and photoluminescence studies of highly crystalline un-annealed ZnO nanorods arrays synthesized by hydrothermal technique. Journal of Luminescence, 2013, 144, 234-240.	3.1	5
240	Influence of catalyst droplet diameter on the growth direction of InP nanowires grown on Si(001) substrate. Applied Physics Letters, 2013, 102, 243113.	3.3	8
241	Structural and compositional characterization of MOVPE GaN thin films transferred from sapphire to glass substrates using chemical lift-off and room temperature direct wafer bonding and GaN wafer scale MOVPE growth on ZnO-buffered sapphire. Journal of Crystal Growth, 2013, 370, 63-67.	1.5	75
242	Multilayered InGaN/GaN structure vs. single InGaN layer for solar cell applications: A comparative study. Acta Materialia, 2013, 61, 6587-6596.	7.9	38
243	Structure and Magnetism of Orthorhombic Epitaxial FeMnAs. Crystal Growth and Design, 2013, 13, 4279-4284.	3.0	2
244	Phase coherent transport in GaAs/AlGaAs core–shellnanowires. Journal of Crystal Growth, 2013, 378, 546-548.	1.5	6
245	Suppression of crack generation in AlGaN/GaN distributed Bragg reflectors grown by MOVPE. Journal of Crystal Growth, 2013, 370, 12-15.	1.5	12
246	Semibulk InGaN: A novel approach for thick, single phase, epitaxial InGaN layers grown by MOVPE. Journal of Crystal Growth, 2013, 370, 57-62.	1.5	47
247	From Excitonic to Photonic Polariton Condensate in a ZnO-Based Microcavity. Physical Review Letters, 2013, 110, 196406.	7.8	162
248	Fabrication and characterization of a room-temperature ZnO polariton laser. Applied Physics Letters, 2013, 102, .	3.3	48
249	Growth of Vertical GaAs Nanowires on an Amorphous Substrate via a Fiber-Textured Si Platform. Nano Letters, 2013, 13, 2743-2747.	9.1	31
250	Polarization properties of single and ensembles of InAs/InP quantum rod nanowires emitting in the telecom wavelengths. Journal of Applied Physics, 2013, 113, 193101.	2.5	7
251	Improvement of the oxidation interface in an Al <scp>G</scp> a <scp>A</scp> s/ <scp>A</scp> l <sub><i>x</i></sub> <scp>O</scp> <sub><i>y</i></sub> waveguide structure by using a Ga <scp>A</scp> s/ <scp>A</scp> l <scp>A</scp> s superlattice. Physica Status Solidi (A) Applications and Materials Science. 2013. 210. 1171-1177.	1.8	0
252	Excitonic properties of wurtzite InP nanowires grown on silicon substrate. Nanotechnology, 2013, 24, 035704.	2.6	24

#	Article	IF	CITATIONS
253	Arsenic Pathways in Self-Catalyzed Growth of GaAs Nanowires. Crystal Growth and Design, 2013, 13, 91-96.	3.0	133
254	InP1â^'xAsx quantum dots in InP nanowires: A route for single photon emitters. Journal of Crystal Growth, 2013, 378, 519-523.	1.5	17
255	Predictive modeling of self-catalyzed III-V nanowire growth. Physical Review B, 2013, 88, .	3.2	158
256	Characteristics of the surface microstructures in thick InGaN layers on GaN. Optical Materials Express, 2013, 3, 1111.	3.0	25
257	Atomic-plane-thick reconstruction across the interface during heteroepitaxial bonding of InP-clad quantum wells on silicon. Applied Physics Letters, 2013, 102, .	3.3	30
258	Heteroepitaxial bonding of Si for hybrid photonic devices. Materials Research Society Symposia Proceedings, 2013, 1510, 1.	0.1	4
259	Band offsets at zincblende-wurtzite GaAs nanowire sidewall surfaces. Applied Physics Letters, 2013, 103, .	3.3	28
260	Towards a monolithically integrated III–V laser on silicon: optimization of multi-quantum well growth on InP on Si. Semiconductor Science and Technology, 2013, 28, 094008.	2.0	16
261	Surface plasmon modulation induced by a direct-current electric field into gallium nitride thin film grown on Si(111) substrate. Applied Physics Letters, 2013, 102, 021905.	3.3	8
262	Evaluation of the surface bonding energy of an InP membrane bonded oxide-free to Si using instrumented nanoindentation. Applied Physics Letters, 2013, 103, 081901.	3.3	13
263	Effect of arsenic on the optical properties of GaSb-based type II quantum wells with quaternary GaInAsSb layers. Journal of Applied Physics, 2013, 114, .	2.5	16
264	Design, Fabrication, and Characterization of Near-Milliwatt-Power RCLEDs Emitting at 390 nm. IEEE Photonics Journal, 2013, 5, 8400709-8400709.	2.0	14
265	Comparison of chemical and laser lift-off for the transfer of InGaN-based p-i-n junctions from sapphire to glass substrates. , 2013, , .		5
266	Fine-tuning of the interface in high-quality epitaxial silicon films deposited by plasma-enhanced chemical vapor deposition at 200 ŰC. Journal of Materials Research, 2013, 28, 1626-1632.	2.6	17
267	Stored elastic energy influence on the elastic–plastic transition of GaAs structures. Journal of Materials Research, 2012, 27, 177-181.	2.6	1
268	Mechanism of Ohmic Cr/Ni/Au contact formation on p-GaN. Journal of Vacuum Science and Technology B:Nanotechnology and Microelectronics, 2012, 30, 022205.	1.2	3
269	Composition and local strain mapping in Au-catalyzed axial Si/Ge nanowires. Nanotechnology, 2012, 23, 395701.	2.6	4
270	Effect of Cl2- and HBr-based inductively coupled plasma etching on InP surface composition analyzed using <i>in situ</i> x-ray photoelectron spectroscopy. Journal of Vacuum Science and Technology A: Vacuum, Surfaces and Films, 2012, 30, .	2.1	16

#	Article	IF	CITATIONS
271	Distributed Bragg reflectors based on diluted boron-based BAIN alloys for deep ultraviolet optoelectronic applications. Applied Physics Letters, 2012, 100, 051101.	3.3	44
272	Kinetics and Statistics of Vapor-Liquid-Solid Growth of III-V Nanowires. Materials Research Society Symposia Proceedings, 2012, 1408, 81.	0.1	0
273	Epitaxial growth of silicon and germanium on (100)-oriented crystalline substrates by RF PECVD at 175 °C. EPJ Photovoltaics, 2012, 3, 30303.	1.6	12
274	Hair Fiber as a Nanoreactor in Controlled Synthesis of Fluorescent Gold Nanoparticles. Nano Letters, 2012, 12, 6212-6217.	9.1	43
275	Atomic-plane-thick reconstruction across the interface during heteroepitaxial bonding of InP-clad quantum wells to Si. , 2012, , .		5
276	Conductance Statistics from a Large Array of Sub-10 nm Molecular Junctions. ACS Nano, 2012, 6, 4639-4647.	14.6	44
277	Colloidal CdSe/CdS Dot-in-Plate Nanocrystals with 2D-Polarized Emission. ACS Nano, 2012, 6, 6741-6750.	14.6	106
278	Growth of vertical and defect free InP nanowires on SrTiO3(001) substrate and comparison with growth on silicon. Journal of Crystal Growth, 2012, 343, 101-104.	1.5	8
279	InAs/InP nanowires grown by catalyst assisted molecular beam epitaxy on silicon substrates. Journal of Crystal Growth, 2012, 344, 45-50.	1.5	17
280	Multi-scale structuration of glasses: Observations of phase separation and nanoscale heterogeneities in glasses by Z-contrast scanning electron transmission microscopy. Journal of Non-Crystalline Solids, 2012, 358, 1257-1262.	3.1	53
281	Effect of diffusion from a lateral surface on the rate of GaN nanowire growth. Semiconductors, 2012, 46, 838-841.	0.5	11
282	Core/Shell Colloidal Semiconductor Nanoplatelets. Journal of the American Chemical Society, 2012, 134, 18591-18598.	13.7	323
283	High density InAlAs/GaAlAs quantum dots for non-linear optics in microcavities. Journal of Applied Physics, 2012, 111, 043107.	2.5	6
284	Growth temperature dependence of exciton lifetime in wurtzite InP nanowires grown on silicon substrates. Applied Physics Letters, 2012, 100, .	3.3	23
285	Protein Transport through a Narrow Solid-State Nanopore at High Voltage: Experiments and Theory. ACS Nano, 2012, 6, 6236-6243.	14.6	126
286	FIB carving of nanopores into suspended graphene films. Microelectronic Engineering, 2012, 97, 311-316.	2.4	36
287	Boron distribution in the core of Si nanowire grown by chemical vapor deposition. Journal of Applied Physics, 2012, 111, 094909.	2.5	44
288	Nanometer-scale, quantitative composition mappings of InGaN layers from a combination of scanning transmission electron microscopy and energy dispersive x-ray spectroscopy. Nanotechnology, 2012, 23, 455707.	2.6	27

#	Article	IF	CITATIONS
289	Investigation of a relaxation mechanism specific to InGaN for improved MOVPE growth of nitride solar cell materials. Physica Status Solidi (A) Applications and Materials Science, 2012, 209, 25-28.	1.8	23
290	Comparative optical studies of InGaAs/GaAs quantum wells grown by MBE on (100) and (311)A GaAs planes. Physica Status Solidi C: Current Topics in Solid State Physics, 2012, 9, 1621-1623.	0.8	7
291	Gold nanocluster distribution on faceted and kinked Si nanowires. Thin Solid Films, 2012, 520, 3304-3308.	1.8	5
292	Effect of postgrowth heat treatment on the structural and optical properties of InP/InAsP/InP nanowires. Semiconductors, 2012, 46, 175-178.	0.5	11
293	Faceting mechanisms of Si nanowires and gold spreading. Journal of Materials Science, 2012, 47, 1609-1613.	3.7	9
294	Mesoscopic scale description of nucleation processes in glasses. Applied Physics Letters, 2011, 99, .	3.3	40
295	Dynamics of Colloids in Single Solid-State Nanopores. Journal of Physical Chemistry B, 2011, 115, 2890-2898.	2.6	86
296	Wurtzite InP/InAs/InP core–shell nanowires emitting at telecommunication wavelengths on Si substrate. Nanotechnology, 2011, 22, 405702.	2.6	24
297	Morphology of self-catalyzed GaN nanowires and chronology of their formation by molecular beam epitaxy. Nanotechnology, 2011, 22, 245606.	2.6	59
298	Confined and Guided Vapor–Liquid–Solid Catalytic Growth of Silicon Nanoribbons: From Nanowires to Structured Silicon-on-Insulator Layers. Engineering Materials, 2011, , 67-89.	0.6	0
299	Structural analysis of site-controlled InAs/InP quantum dots. Journal of Crystal Growth, 2011, 334, 37-39.	1.5	3
300	New generation of Distributed Bragg Reflectors based on BAIN/AIN structures for deep UV-optoelectronic applications. , 2011, , .		1
301	Synthesis of long group IV semiconductor nanowires by molecular beam epitaxy. Nanoscale Research Letters, 2011, 6, 113.	5.7	18
302	Large Array of Subâ€10â€nm Singleâ€Grain Au Nanodots for use in Nanotechnology. Small, 2011, 7, 2607-2613.	10.0	31
303	Direct epitaxial growth of InP based heterostructures on SrTiO3/Si(001) crystalline templates. Microelectronic Engineering, 2011, 88, 469-471.	2.4	1
304	Origin of light scattering in ytterbium doped calcium fluoride transparent ceramic for high power lasers. Journal of the European Ceramic Society, 2011, 31, 1619-1630.	5.7	98
305	Deep structural analysis of novel BGaN material layers grown by MOVPE. Journal of Crystal Growth, 2011, 315, 288-291.	1.5	31
306	Structural and optical properties of nanodots, nanowires, and multi-quantum wells of III-nitride grown by MOVPE nano-selective area growth. Journal of Crystal Growth, 2011, 315, 160-163.	1.5	31

#	Article	IF	CITATIONS
307	GaP/GaAs1â^'xPx nanowires fabricated with modulated fluxes: A step towards the realization of superlattices in a single nanowire. Journal of Crystal Growth, 2011, 323, 293-296.	1.5	23
308	Tuning the structural properties of InAs nanocrystals grown by molecular beam epitaxy on silicon dioxide. Journal of Crystal Growth, 2011, 321, 1-7.	1.5	1
309	Gold anchoring on Si sawtooth faceted nanowires. Europhysics Letters, 2011, 95, 18004.	2.0	9
310	Efficient photogeneration of charge carriers in silicon nanowires with a radial doping gradient. Nanotechnology, 2011, 22, 315710.	2.6	14
311	Quasi one-dimensional transport in single GaAs/AlGaAs core-shell nanowires. Applied Physics Letters, 2011, 98, .	3.3	22
312	InGaAs Quantum Dots Grown by Molecular Beam Epitaxy for Light Emission on Si Substrates. Journal of Nanoscience and Nanotechnology, 2011, 11, 9153-9159.	0.9	4
313	High-aspect-ratio inductively coupled plasma etching of InP using SiH4/Cl2: Avoiding the effect of electrode coverplate material. Journal of Vacuum Science and Technology B:Nanotechnology and Microelectronics, 2011, 29, 020601.	1.2	5
314	Growth-in-place deployment of in-plane silicon nanowires. Applied Physics Letters, 2011, 99, .	3.3	38
315	Last advances in Yb3+doped CaF 2 ceramics synthesis. , 2011, , .		3
316	Addition of Si-Containing Gases for Anisotropic Etching of III–V Materials in Chlorine-Based Inductively Coupled Plasma. Japanese Journal of Applied Physics, 2011, 50, 08JE02.	1.5	3
317	Selective growth of site-controlled Quantum Dots. , 2011, , .		Ο
318	Addition of Si-Containing Gases for Anisotropic Etching of III–V Materials in Chlorine-Based Inductively Coupled Plasma. Japanese Journal of Applied Physics, 2011, 50, 08JE02.	1.5	2
319	Growth of III-Arsenide/Phosphide Nanowires by Molecular Beam Epitaxy. , 2011, , 68-88.		1
320	Growth of III-Arsenide/Phosphide Nanowires by Molecular Beam Epitaxy. , 2011, , 68-88.		0
321	Quantum optics with single nanowire quantum dots. , 2010, , .		1
322	Polarization Properties of Columnar Quantum Dots: Effects of Aspect Ratio and Compositional Contrast. IEEE Journal of Quantum Electronics, 2010, 46, 197-204.	1.9	19
323	Direct FIB fabrication and integration of "single nanopore devices―for the manipulation of macromolecules. Microelectronic Engineering, 2010, 87, 1300-1303.	2.4	33
324	Confined VLS growth and structural characterization of silicon nanoribbons. Microelectronic Engineering, 2010, 87, 1522-1526.	2.4	7

#	Article	IF	CITATIONS
325	Elastic anisotropy of polycrystalline Au films: Modeling and respective contributions of X-ray diffraction, nanoindentation and Brillouin light scattering. Acta Materialia, 2010, 58, 4998-5008.	7.9	36
326	Effects of substrates and catalysts compositions on the crystalline quality of InP Nanowires grown on SrTiO3 (001), Si(001) and InP (111). Materials Research Society Symposia Proceedings, 2010, 1258, 1.	0.1	0
327	Tailoring nanopores for efficient sensing of different biomolecules. Materials Research Society Symposia Proceedings, 2010, 1253, 33.	0.1	1
328	Optically Active Defects in an InAsP/InP Quantum Well Monolithically Integrated on SrTiO3 (001). Materials Research Society Symposia Proceedings, 2010, 1252, 1.	0.1	2
329	Nano-Patterning of Graphene Structures Using Highly Focused Beams of Gallium Ions. Materials Research Society Symposia Proceedings, 2010, 1259, 1.	0.1	2
330	Quantum well infrared photodetectors hardiness to the nonideality of the energy band profile. Journal of Applied Physics, 2010, 107, .	2.5	3
331	Nucleation Antibunching in Catalyst-Assisted Nanowire Growth. Physical Review Letters, 2010, 104, 135501.	7.8	100
332	Growth kinetics of a single <mml:math <br="" xmlns:mml="http://www.w3.org/1998/Math/MathML">display="inline"&gt;<mml:msub><mml:mtext>InP</mml:mtext><mml:mrow><mml:mn>1</mml:mn><ml:mo>â^'&lt; Physical Review B, 2010, 81, .</ml:mo></mml:mrow></mml:msub></mml:math>	/mænde:mo>	<n<b>86nl:mi&gt;x&lt;</n<b>
333	Effects of using As2 and As4 on the optical properties of InGaAs quantum rods grown by molecular beam epitaxy. Journal of Applied Physics, 2010, 108, 103522.	2.5	6
334	Type II heterostructures formed by zinc-blende inclusions in InP and GaAs wurtzite nanowires. Applied Physics Letters, 2010, 97, 041910.	3.3	54
335	Interface roughness transport in terahertz quantum cascade detectors. Applied Physics Letters, 2010, 96, 061111.	3.3	15
336	Crystal Phase Quantum Dots. Nano Letters, 2010, 10, 1198-1201.	9.1	233
337	Growth, structure and phase transitions of epitaxial nanowires of III-V semiconductors. Journal of Physics: Conference Series, 2010, 209, 012002.	0.4	14
338	Time-resolved spectroscopy of InAsP/InP(001) quantum dots emitting near 2â€,μm. Applied Physics Letters, 2010, 97, 131907.	3.3	13
339	Optical and structural properties of INP nanowires grown on silicon substrate. , 2010, , .		0
340	Nanowires for quantum optics. , 2010, , .		1
341	Localisation of silicon nanowires grown by UHV-CVD in (111)-oriented apertures opened in Si (001). IOP Conference Series: Materials Science and Engineering, 2009, 6, 012015.	0.6	2
342	Structure of annealed nanoindentations in n- and p-doped (001)GaAs. Journal of Applied Physics, 2009, 106, .	2.5	2

#	Article	IF	CITATIONS
343	Twin formation during the growth of InP on SrTiO3. Applied Physics Letters, 2009, 94, 231902.	3.3	9
344	Control of polarization and dipole moment in low-dimensional semiconductor nanostructures. Applied Physics Letters, 2009, 95, 221116.	3.3	14
345	Optically active defects in an InAsP/InP quantum well monolithically grown on SrTiO3(001). Applied Physics Letters, 2009, 95, .	3.3	14
346	Accommodation at the interface of highly dissimilar semiconductor/oxide epitaxial systems. Physical Review B, 2009, 80, .	3.2	42
347	Orientation dependent emission properties of columnar quantum dash laser structures. Applied Physics Letters, 2009, 94, 241113.	3.3	13
348	Surface-emitting quantum cascade lasers with metallic photonic-crystal resonators. Applied Physics Letters, 2009, 94, 221101.	3.3	24
349	Epitaxial growth and picosecond carrier dynamics at 1.55µm of GaInAs/GaInNAs superlattices. , 2009, , .		0
350	Time-multiplexed, inductively coupled plasma process with separate SiCl4 and O2 steps for etching of GaAs with high selectivity. Journal of Vacuum Science & Technology B, 2009, 27, 2270-2279.	1.3	11
351	Epitaxial growth and picosecond carrier dynamics of GalnAs/GalnNAs superlattices. Applied Physics Letters, 2009, 95, 141910.	3.3	6
352	Inductively coupled plasma etching of GaAs suspended photonic crystal cavities. Journal of Vacuum Science & Technology B, 2009, 27, 1909-1914.	1.3	14
353	Crystal orientation of GaAs islands grown on SrTiO3 (001) by molecular beam epitaxy. Applied Physics Letters, 2009, 95, 011907.	3.3	10
354	Surface-plasmon distributed-feedback quantum cascade lasers operating pulsed, room temperature. Applied Physics Letters, 2009, 95, 091105.	3.3	10
355	Electronic structure properties of the In(Ga)As/GaAs quantum dot–quantum well tunnel-injection system. Semiconductor Science and Technology, 2009, 24, 085011.	2.0	3
356	Si Incorporation in InP Nanowires Grown by Au-Assisted Molecular Beam Epitaxy. Journal of Nanomaterials, 2009, 2009, 1-7.	2.7	11
357	One Step Nano-Selective Area Growth of Localized InAs/InP Quantum Dots For Single Photon Source Applications. Materials Research Society Symposia Proceedings, 2009, 1228, 120701.	0.1	0
358	Direct FIB fabrication and integration of "single nanopore devices―for the manipulation of macromolecules. Materials Research Society Symposia Proceedings, 2009, 1191, 78.	0.1	2
359	Exploration of the ultimate patterning potential achievable with focused ion beams. Ultramicroscopy, 2009, 109, 457-462.	1.9	17
360	Doping influence on the nanoindentation response of GaAs. Physica Status Solidi C: Current Topics in Solid State Physics, 2009, 6, 1841-1846.	0.8	1

#	Article	IF	CITATIONS
361	Synthesis and optical characterizations of Yb-doped CaF2 ceramics. Optical Materials, 2009, 31, 750-753.	3.6	113
362	High yield syntheses of reactive fluoride K1â^'x(Y,Ln)xF1+2x nanoparticles. Optical Materials, 2009, 31, 1177-1183.	3.6	15
363	Growth and structural characterization of GaAs/GaAsSb axial heterostructured nanowires. Journal of Crystal Growth, 2009, 311, 1847-1850.	1.5	23
364	Influence of the surface reconstruction on the growth of InP on SrTiO3(001). Journal of Crystal Growth, 2009, 311, 1042-1045.	1.5	16
365	Optimization of 1550nm InAs/InP Quantum Dash and Quantum Dot based semiconductor optical amplifier. , 2009, , .		1
366	A semiconductor laser device for the generation of surface-plasmons upon electrical injection. Optics Express, 2009, 17, 9391.	3.4	26
367	Silicon Nanowires Coated with Silver Nanostructures as Ultrasensitive Interfaces for Surface-Enhanced Raman Spectroscopy. ACS Applied Materials & Interfaces, 2009, 1, 1396-1403.	8.0	133
368	Role of nonlinear effects in nanowire growth and crystal phase. Physical Review B, 2009, 80, .	3.2	90
369	Columnar Quantum Dashes for polarization insensitive semiconductor optical amplifiers. , 2009, , .		1
370	Mid/far-infrared semiconductor devices exploiting plasmonic effects. Proceedings of SPIE, 2009, , .	0.8	0
371	Potential of semiconductor nanowires for single photon sources. Proceedings of SPIE, 2009, , .	0.8	4
372	Challenges and Opportunities for Focused Ion Beam Processing at the Nano-scale. Microscopy and Microanalysis, 2009, 15, 320-321.	0.4	0
373	Nanoindentation-induced structural phase transformations in crystalline and amorphous germanium. International Journal of Nano and Biomaterials, 2009, 2, 91.	0.1	Ο
374	Single photon sources using InAs/InP quantum dots. Proceedings of SPIE, 2009, , .	0.8	1
375	Surface emitting photonic crystal mid-infrared quantum cascade lasers. , 2009, , .		Ο
376	Polarization dependence of electroluminescence from closely-stacked and columnar quantum dots. Optical and Quantum Electronics, 2008, 40, 239-248.	3.3	25
377	Influence of recapture on the emission statistics of short radiative lifetime quantum dots. Physica Status Solidi C: Current Topics in Solid State Physics, 2008, 5, 2520-2523.	0.8	1
378	GaN/AlN freeâ€standing nanowires grown by molecular beam epitaxy. Physica Status Solidi C: Current Topics in Solid State Physics, 2008, 5, 1556-1558.	0.8	16

#	Article	IF	CITATIONS
379	De-relaxation of plastically relaxed InAs/GaAs quantum dots during the growth of a GaAs encapsulation layer. Journal of Crystal Growth, 2008, 310, 536-540.	1.5	3
380	One-step nano-selective area growth (nano-SAG) of localized InAs/InP quantum dots: First step towards single-photon source applications. Journal of Crystal Growth, 2008, 310, 3413-3415.	1.5	9
381	A new way to integrate solid state nanopores for translocation experiments. Microelectronic Engineering, 2008, 85, 1311-1313.	2.4	1
382	Optics with single nanowires. Comptes Rendus Physique, 2008, 9, 804-815.	0.9	21
383	Structure of nanoindentations in heavily n- and p-doped (001) GaAs. Acta Materialia, 2008, 56, 1417-1426.	7.9	13
384	Epitaxial growth of high-lº oxides on silicon. Thin Solid Films, 2008, 517, 197-200.	1.8	7
385	In situ generation of indium catalysts to grow crystalline silicon nanowires at low temperature on ITO. Journal of Materials Chemistry, 2008, 18, 5187.	6.7	81
386	Heterostructure formation in nanowhiskers via diffusion mechanism. Technical Physics Letters, 2008, 34, 750-753.	0.7	2
387	Controlling the Aspect Ratio of Quantum Dots: From Columnar Dots to Quantum Rods. IEEE Journal of Selected Topics in Quantum Electronics, 2008, 14, 1204-1213.	2.9	17
388	Photonic crystal nanolasers with controlled spontaneous emission. Proceedings of SPIE, 2008, , .	0.8	0
389	Tuning InAs/InP(001) quantum dot emission from 1.55 to 2 μm by varying cap-layer growth rate in metalorganic vapor phase epitaxy. , 2008, , .		0
390	Anisotropic and Smooth Inductively Coupled Plasma Etching of III-V Laser Waveguides Using HBr-O[sub 2] Chemistry. Journal of the Electrochemical Society, 2008, 155, H778.	2.9	24
391	Preparation and up-conversion luminescence of 8 nm rare-earth doped fluoride nanoparticles. Optics Express, 2008, 16, 14544.	3.4	41
392	Wurtzite to Zinc Blende Phase Transition in GaAs Nanowires Induced by Epitaxial Burying. Nano Letters, 2008, 8, 1638-1643.	9.1	63
393	One step Nano Selective Area Growth of localized InAs/InP quantum dots for single photon source applications. , 2008, , .		Ο
394	Monolithic integration of InP based heterostructures on silicon using crystalline Gd <inf>2</inf> O <inf>3</inf> buffers. , 2008, , .		0
395	InAsP/InP(001) quantum dots emitting at 1.55 $\hat{l}$ $4$ m grown by metalorganic vapor phase epitaxy. , 2008, , .		0
396	Influence of surface reconstructions on the shape of InAs quantum dots grown on InP(001). , 2008, , .		1

23

#	Article	IF	CITATIONS
397	Zinc blende GaAsSb nanowires grown by molecular beam epitaxy. Nanotechnology, 2008, 19, 275605.	2.6	53
398	Mechanism of anisotropy during inductively coupled plasma (ICP) etching of inp-based heterostructures for the fabrication of photonic devices. , 2008, , .		0
399	Surface-plasmon distributed-feedback mid-infrared quantum cascade lasers based on hybrid plasmon/air-guided modes. , 2008, , .		1
400	Spontaneous compliance of the InPâ^•SrTiO3 heterointerface. Applied Physics Letters, 2008, 92, .	3.3	36
401	Surface-plasmon distributed-feedback mid-infrared quantum cascade lasers based on hybrid plasmon/air-guided modes. Electronics Letters, 2008, 44, 807.	1.0	12
402	Growth and Characterization of Wurtzite GaAs Nanowires with Defect-Free Zinc Blende GaAsSb Inserts. Nano Letters, 2008, 8, 4459-4463.	9.1	112
403	Exploration of the Ultimate Patterning Potential Achievable with Focused Ion Beams. Materials Research Society Symposia Proceedings, 2008, 1089, 30101.	0.1	1
404	Nanoindentation response of a thin InP membrane. Journal Physics D: Applied Physics, 2008, 41, 074003.	2.8	2
405	Sidewall passivation assisted by a silicon coverplate during Cl2–H2 and HBr inductively coupled plasma etching of InP for photonic devices. Journal of Vacuum Science & Technology B, 2008, 26, 666-674.	1.3	37
406	Smooth sidewall in InP-based photonic crystal membrane etched by N[sub 2]-based inductively coupled plasma. Journal of Vacuum Science & Technology B, 2008, 26, 1326.	1.3	19
407	InP nanowires grown on Silicon and SrTiO <inf>3</inf> by VLS assisted MBE. , 2008, , .		1
408	Dipole orientation in a Quantum Rod. , 2008, , .		0
409	Columnar quantum dashes for an active region in polarization independent semiconductor optical amplifiers at 1.551¼m. Applied Physics Letters, 2008, 93, .	3.3	23
410	Competition between InP and In2O3 islands during the growth of InP on SrTiO3. Journal of Applied Physics, 2008, 104, 033509.	2.5	4
411	Photoluminescence from a single InGaAs epitaxial quantum rod. Applied Physics Letters, 2008, 92, 021901.	3.3	22
412	Growth-interruption-induced low-density InAs quantum dots on GaAs. Journal of Applied Physics, 2008, 104, .	2.5	23
413	Metamorphic approach to single quantum dot emission at 1.55μm on GaAs substrate. Journal of Applied Physics, 2008, 103, .	2.5	50
414	Self-assembled Ge nanocrystals on BaTiO3â^•SrTiO3â^•Si(001). Applied Physics Letters, 2008, 92, .	3.3	19

#	Article	IF	CITATIONS
415	Metal organic vapor phase epitaxy of InAsP/InP(001) quantum dots for 1.55î¼m applications: Growth, structural, and optical properties. Journal of Applied Physics, 2008, 104, 043504.	2.5	27
416	Shape-engineered epitaxial InGaAs quantum rods for laser applications. Applied Physics Letters, 2008, 92, 121102.	3.3	23
417	Scanning tunneling spectroscopy of cleaved InAs/GaAs quantum dots at low temperatures. Physical Review B, 2008, 77, .	3.2	33
418	Epitaxial growth of quantum rods with high aspect ratio and compositional contrast. Journal of Applied Physics, 2008, 104, .	2.5	13
419	Directional growth of Ge on GaAs at 175°C using plasma-generated nanocrystals. Applied Physics Letters, 2008, 92, 103108.	3.3	15
420	Semiconductor nanowires in InP and related material systems: MBE growth and properties. , 2008, , .		1
421	Recent developments of InP-based quantum dashes for directly modulated lasers and semiconductor optical amplifiers. Proceedings of SPIE, 2008, , .	0.8	1
422	Surface-Plasmons on Structured Metallic Surfaces: Theoretical Analysis, Applications to Mid-Infrared Quantum Cascade Lasers and a-SNOM Survey. , 2008, , .		0
423	Towards polarization insensitive semiconductor optical amplifiers using InAs/GaAs columnar quantum dots. , 2008, , .		1
424	Nano-FIB from Research to Applications — a European Scalpel for Nanosciences. Springer Proceedings in Physics, 2008, , 431-440.	0.2	0
425	Telecom-wavelength single-photon sources for quantum communications. Journal of Physics Condensed Matter, 2007, 19, 225005.	1.8	10
426	Local electronic transport through InAs/InP(0 0 1) quantum dots capped with a thin InP layer studied by an AFM conductive probe. Semiconductor Science and Technology, 2007, 22, 755-762.	2.0	3
427	Optical and electronic properties of GaAs-based structures with columnar quantum dots. Applied Physics Letters, 2007, 90, 181933.	3.3	13
428	Density of InAsâ^•InP(001) quantum dots grown by metal-organic vapor phase epitaxy: Independent effects of InAs and cap-layer growth rates. Applied Physics Letters, 2007, 91, .	3.3	14
429	Structural and optical properties of low-density and In-rich InAsâ^•GaAs quantum dots. Journal of Applied Physics, 2007, 101, 024918.	2.5	38
430	Submicron-diameter semiconductor pillar microcavities with very high quality factors. Applied Physics Letters, 2007, 90, 091120.	3.3	29
431	Growth of crystalline γâ€Al2O3 on Si by molecular beam epitaxy: Influence of the substrate orientation. Journal of Applied Physics, 2007, 102, 024101.	2.5	22
432	Modulation spectroscopy characterization of InAs/GaInAsP/InP quantum dash laser structures. , 2007, 6481, 52.		2

#	Article	IF	CITATIONS
433	Mechanical response of a single and released InP membrane. Materials Research Society Symposia Proceedings, 2007, 1049, 1.	0.1	0
434	Thermodynamic analysis of the shape, anisotropy and formation process of InAs/InP(001) quantum dots and quantum sticks grown by metalorganic vapor phase epitaxy. Surface Science, 2007, 601, 2765-2768.	1.9	3
435	Synthesis of silicon nanocrystals in silane plasmas for nanoelectronics and large area electronic devices. Journal Physics D: Applied Physics, 2007, 40, 2258-2266.	2.8	72
436	Au-assisted molecular beam epitaxy of InAs nanowires: Growth and theoretical analysis. Journal of Applied Physics, 2007, 102, 094313.	2.5	136
437	Growth of GaN free-standing nanowires by plasma-assisted molecular beam epitaxy: structural and optical characterization. Nanotechnology, 2007, 18, 385306.	2.6	109
438	InAs nanocrystals on SiO2â^•Si by molecular beam epitaxy for memory applications. Applied Physics Letters, 2007, 91, 133114.	3.3	16
439	Wetting layer states of InAsâ^•GaAs self-assembled quantum dot structures: Effect of intermixing and capping layer. Journal of Applied Physics, 2007, 101, 063539.	2.5	31
440	Fast radiative quantum dots: From single to multiple photon emission. Applied Physics Letters, 2007, 90, 223118.	3.3	26
441	Why Does Wurtzite Form in Nanowires of III-V Zinc Blende Semiconductors?. Physical Review Letters, 2007, 99, 146101.	7.8	669
442	Processing of InP-Based Shallow Ridge Laser Waveguides Using a HBr ICP Plasma. Indium Phosphide and Related Materials Conference (IPRM), IEEE International Conference on, 2007, , .	0.0	0
443	InAs/InP Quantum Dash Based Electro Optic Modulator with Over 70 NM Bandwidth at 1.55 μM. , 2007, , .		1
444	Polarization dependence study of electroluminescence and absorption from InAsâ^•GaAs columnar quantum dots. Applied Physics Letters, 2007, 91, .	3.3	39
445	Monolithic integration of InP based heterostructures on silicon using crystalline Gd2O3 buffers. Applied Physics Letters, 2007, 91, .	3.3	53
446	Tolerance to Optical Feedback of 10 GBPs Quantum-Dash Based Lasers Emitting at 1.55 μm. , 2007, , .		2
447	Growth and characterization of InAs columnar quantum dots on GaAs substrate. Journal of Applied Physics, 2007, 102, 033502.	2.5	28
448	Growth and Characterization of InP Nanowires with InAsP Insertions. Nano Letters, 2007, 7, 1500-1504.	9.1	110
449	Study of radial growth rate and size control of silicon nanocrystals in square-wave-modulated silane plasmas. Applied Physics Letters, 2007, 91, 111501.	3.3	17
450	InAs/InP(001) Quantum Dots And Quantum Sticks Grown By MOVPE: Shape, Anisotropy And Formation Process. AIP Conference Proceedings, 2007, , .	0.4	0

#	Article	IF	CITATIONS
451	Organometallic precursors as catalyst to grow three-dimensional micro/nanostructures: Spheres, clusters & wires. Surface and Coatings Technology, 2007, 201, 9104-9108.	4.8	6
452	Large intrinsic birefringence in zinc-blende based artificial semiconductors. Comptes Rendus Physique, 2007, 8, 1174-1183.	0.9	1
453	Sub-5nm FIB direct patterning of nanodevices. Microelectronic Engineering, 2007, 84, 779-783.	2.4	117
454	Development of robust interfaces based on crystalline γ-Al2O3(001) for subsequent deposition of amorphous high-lº oxides. Microelectronic Engineering, 2007, 84, 2243-2246.	2.4	20
455	TEM-nanoindentation studies of semiconducting structures. Micron, 2007, 38, 377-389.	2.2	14
456	Rare-earth doped oxyfluoride glass-ceramics and fluoride ceramics: Synthesis and optical properties. Optical Materials, 2007, 29, 1263-1270.	3.6	81
457	Growth of InAs bilayer quantum dots for long-wavelength laser emission on GaAs. Journal of Crystal Growth, 2007, 301-302, 959-962.	1.5	19
458	GaAs nanowires formed by Au-assisted molecular beam epitaxy: Effect of growth temperature. Journal of Crystal Growth, 2007, 301-302, 853-856.	1.5	73
459	Nanoindentation response of compound semiconductors. Physica Status Solidi C: Current Topics in Solid State Physics, 2007, 4, 3002-3009.	0.8	4
460	Modulated reflectivity probing of quantum dot and wetting layer states in InAs/GaInAsP/InP quantum dot laser structures. Physica Status Solidi (A) Applications and Materials Science, 2007, 204, 496-499.	1.8	4
461	Synthesis and photoluminescence properties of silicon nanowires treated by high-pressure water vapor annealing. Physica Status Solidi (A) Applications and Materials Science, 2007, 204, 1302-1306.	1.8	26
462	Advances in fluoride-based ceramic laser media. , 2007, , .		0
463	Towards A Mid-Infrared Polaron Laser Using InAs/GaAs Self-Assembled Quantum Dots. AIP Conference Proceedings, 2007, , .	0.4	Ο
464	Temperature conditions for GaAs nanowire formation by Au-assisted molecular beam epitaxy. Nanotechnology, 2006, 17, 4025-4030.	2.6	107
465	Low density of self-assembled InAs quantum dots grown by solid-source molecular beam epitaxy on InP(001). Applied Physics Letters, 2006, 89, 123112.	3.3	19
466	Thermodynamical analysis of the shape and size dispersion ofInAsâ^•InP(001)quantum dots. Physical Review B, 2006, 73, .	3.2	15
467	Magnetic properties and domain structure of (Ga,Mn)As films with perpendicular anisotropy. Physical Review B, 2006, 73, .	3.2	62
468	Influence of deposition parameters and post-deposition plasma treatments on the photoluminescence of polymorphous silicon carbon alloys. Journal of Non-Crystalline Solids, 2006, 352, 1357-1360.	3.1	11

#	Article	IF	CITATIONS
469	Effect of cap-layer growth rate on morphology and luminescence of InAsâ^•InP(001) quantum dots grown by metal-organic vapor phase epitaxy. Journal of Applied Physics, 2006, 100, 033508.	2.5	13
470	Synthesis of Fluoride Nanoparticles in Non-Aqueous Nanoreactors. Luminescence Study of Eu3+:CaF2. Zeitschrift Fur Anorganische Und Allgemeine Chemie, 2006, 632, 1538-1543.	1.2	22
471	InAs/InP(001) quantum dots and quantum sticks grown by MOVPE: shape, anisotropy and formation process. Physica Status Solidi C: Current Topics in Solid State Physics, 2006, 3, 3928-3931.	0.8	0
472	InAs(Sb) quantum dots grown on GaAs by MBE. Physica Status Solidi C: Current Topics in Solid State Physics, 2006, 3, 3997-4000.	0.8	5
473	Cavity QED with a single QD inside an optical microcavity. Physica Status Solidi (B): Basic Research, 2006, 243, 3879-3884.	1.5	5
474	Towards a mid-infrared polaron laser using InAs/GaAs self-assembled quantum dots. Physica Status Solidi (B): Basic Research, 2006, 243, 3895-3899.	1.5	0
475	Influence of Ce3+ doping on the structure and luminescence of Er3+-doped transparent glass-ceramics. Optical Materials, 2006, 28, 638-642.	3.6	28
476	Er3+-doped PbF2: Comparison between nanocrystals in glass-ceramics and bulk single crystals. Journal of Solid State Chemistry, 2006, 179, 1995-2003.	2.9	103
477	Structural and photoluminescence studies of InAsN quantum dots grown on GaAs by MBE. Journal of Crystal Crowth, 2006, 290, 80-86.	1.5	16
478	Oxide glass used as inorganic template for fluorescent fluoride nanoparticles synthesis. Optical Materials, 2006, 28, 1401-1404.	3.6	29
479	Elastic properties of polycrystalline gold thin films: Simulation and X-ray diffraction experiments. Surface and Coatings Technology, 2006, 201, 4300-4304.	4.8	8
480	Synthesis and optical characterizations of undoped and rare-earth-doped CaF2 nanoparticles. Journal of Solid State Chemistry, 2006, 179, 2636-2644.	2.9	110
481	Focused ion beam sculpted membranes for nanoscience tooling. Microelectronic Engineering, 2006, 83, 1474-1477.	2.4	54
482	Neutral and charged multi-exciton complexes in single InAs quantum dots grown on InP(001). Nanotechnology, 2006, 17, 1831-1834.	2.6	9
483	Subpicosecond pulse generation at 134â€CHz and low radiofrequency spectral linewidth in quantum dash-based Fabry-Perot lasers emitting at 1.5â€[micro sign]m. Electronics Letters, 2006, 42, 91.	1.0	27
484	1.43â€[micro sign]m InAs bilayer quantum dot lasers on GaAs substrate. Electronics Letters, 2006, 42, 638.	1.0	19
485	Metal-insulator Transition and Magnetic Domains in (Ga,Mn)As Epilayers. Materials Research Society Symposia Proceedings, 2006, 941, 1.	0.1	1
486	Synthesis and Optical Properties of Silicon Oxide Nanowires. Materials Research Society Symposia Proceedings, 2006, 958, 1.	0.1	0

#	Article	IF	CITATIONS
487	Subpicosecond pulse generation at 134GHz using a quantum-dash-based Fabry-Perot laser emitting at 1.561¼m. Applied Physics Letters, 2006, 88, 241105.	3.3	93
488	Initial stage of the overgrowth of InP on InAsâ^•InP(001) quantum dots: Formation of InP terraces driven by preferential nucleation on quantum dot edges. Applied Physics Letters, 2006, 89, 031923.	3.3	14
489	Imaging the electric properties of InAsâ^•InP(001) quantum dots capped with a thin InP layer by conductive atomic force microscopy: Evidence of memory effect. Applied Physics Letters, 2006, 89, 112115.	3.3	18
490	Structural properties of epitaxial SrTiO3 thin films grown by molecular beam epitaxy on Si(001). Journal of Applied Physics, 2006, 100, 124109.	2.5	67
491	Vapor-liquid-solid mechanisms: Challenges for nanosized quantum cluster/dot/wire materials. Journal of Applied Physics, 2006, 100, 044315.	2.5	46
492	Pseudomorphic molecular beam epitaxy growth of Î <sup>3</sup> -Al2O3(001) on Si(001) and evidence for spontaneous lattice reorientation during epitaxy. Applied Physics Letters, 2006, 89, 232907.	3.3	32
493	Microphotoluminescence of exciton and biexciton around 1.5μm from a single InAsâ^•InP(001) quantum dot. Applied Physics Letters, 2006, 88, 133101.	3.3	17
494	Microphotoluminescence around 1.5 μm from a single InAs/InP(001) quantum dot grown by MOVPE , 2006, , .		0
495	Strong linear polarization induced by a longitudinal magnetic field in II-VI semimagnetic semiconductor layers. Physical Review B, 2006, 74, .	3.2	Ο
496	Indium incorporation in In-richInxGa1â^'xAsâ^•GaAslayers grown by low-pressure metalorganic vapor-phase epitaxy and its influence on the growth of self-assembled quantum dots. Physical Review B, 2006, 73, .	3.2	1
497	Effect of layer stacking and p-type doping on the performance of InAsâ^•InP quantum-dash-in-a-well lasers emitting at 1.55μm. Applied Physics Letters, 2006, 89, 241123.	3.3	31
498	Thermodynamic description of the competition between quantum dots and quantum dashes during metalorganic vapor phase epitaxy in theInAsâ^•InP(001)system: Experiment and theory. Physical Review B, 2006, 74, .	3.2	15
499	Elastic behavior of polycrystalline thin films inferred from in situ micromechanical testing and modeling. Applied Physics Letters, 2006, 89, 061911.	3.3	21
500	Quality Factor of Micropillar Cavity. , 2006, , .		0
501	Indentation behaviour of (011) thin films of Ill–V semiconductors: polarity effect differences between GaAs and InP. International Journal of Materials Research, 2006, 97, 1230-1234.	0.3	0
502	Buried dislocation networks for the controlled growth of III–V semiconductor nanostructures. Journal of Crystal Growth, 2005, 275, e1647-e1653.	1.5	1
503	Stress-driven self-ordering of III–V nanostructures. Journal of Crystal Growth, 2005, 275, e2245-e2249.	1.5	3
504	CSMBE growth of GaInAsP/InP 1.3μm-TM-lasers for monolithic integration with optical waveguide isolator. Journal of Crystal Growth, 2005, 278, 709-713.	1.5	4

#	Article	IF	CITATIONS
505	An indentation method to measure the CRSS of semiconducting materials at elevated temperature. Materials Science & Engineering A: Structural Materials: Properties, Microstructure and Processing, 2005, 400-401, 451-455.	5.6	0
506	Mechanical response of wall-patterned GaAs surface. Acta Materialia, 2005, 53, 1907-1912.	7.9	11
507	Luminescence of polymorphous silicon carbon alloys. Optical Materials, 2005, 27, 953-957.	3.6	21
508	Conservative indentation flow throughout thin (011) InP foils. Journal of Materials Science, 2005, 40, 3809-3811.	3.7	0
509	Stress-engineered orderings of self-assembled III-V semiconductor nanostructures. Physica Status Solidi C: Current Topics in Solid State Physics, 2005, 2, 1245-1250.	0.8	1
510	Dislocation networks adapted to order the growth of III-V semiconductor nanostructures. Physica Status Solidi C: Current Topics in Solid State Physics, 2005, 2, 1933-1937.	0.8	4
511	Polarity influence on the nanoindentation response of GaAs. Physica Status Solidi C: Current Topics in Solid State Physics, 2005, 2, 2004-2009.	0.8	2
512	Indentation deformation of thin {111} GaAs and InSb foils: influence of polarity. Philosophical Magazine Letters, 2005, 85, 1-12.	1.2	4
513	Deviation of the mechanical response of Wall-patterned (001) GaAs Surface: a central-plastic-zone criterion. Materials Research Society Symposia Proceedings, 2005, 904, 1.	0.1	0
514	Growth of nanometric CuGaxOystructures on copper substrates. Nanotechnology, 2005, 16, 2790-2793.	2.6	5
515	Polarity influence on the indentation punching of thin {111} GaAs foils at elevated temperatures. Journal Physics D: Applied Physics, 2005, 38, 1140-1147.	2.8	5
516	Reactive-ion etching of high-Q and submicron-diameter GaAsâ^•AlAs micropillar cavities. Journal of Vacuum Science & Technology an Official Journal of the American Vacuum Society B, Microelectronics Processing and Phenomena, 2005, 23, 2499.	1.6	19
517	Determination of In(Ga)As/GaAs quantum dot composition profile. AIP Conference Proceedings, 2005, ,	0.4	0
518	Electroabsorption spectroscopy of Geâ^•Si self-assembled islands. Journal of Applied Physics, 2005, 97, 083525.	2.5	1
519	Optical and structural investigation of In1â^'xGaxP free-standing microrods. Journal of Applied Physics, 2005, 98, 053506.	2.5	5
520	InAsâ^•InP(001) quantum dots emitting at 1.55μm grown by low-pressure metalorganic vapor-phase epitaxy. Applied Physics Letters, 2005, 87, 253114.	3.3	33
521	Nanoindentation response of a single micrometer-sized GaAs wall. Applied Physics Letters, 2005, 86, 163107.	3.3	4
522	Mid-infrared intersublevel absorption of vertically electronically coupled InAs quantum dots. Applied Physics Letters, 2005, 87, 173113.	3.3	21

#	Article	IF	CITATIONS
523	Nucleation efficiency of erbium and ytterbium fluorides in transparent oxyfluoride glass-ceramics. Journal of Materials Research, 2005, 20, 472-481.	2.6	50
524	Indentation Crystallization and Phase Transformation of Amorphous Germanium. Materials Research Society Symposia Proceedings, 2005, 904, 1.	0.1	0
525	Analysis of vapor-liquid-solid mechanism in Au-assisted GaAs nanowire growth. Applied Physics Letters, 2005, 87, 203101.	3.3	249
526	Effect of CeF3Addition on the Nucleation and Up-Conversion Luminescence in Transparent Oxyfluoride Glassâ^'Ceramics. Chemistry of Materials, 2005, 17, 2216-2222.	6.7	74
527	GaNAsSb Alloy and Its Potential for Device Applications. , 2005, , 471-493.		5
528	Transformation de phase dans un film de germanium amorphe induite par nano-indentation. Materiaux Et Techniques, 2005, 93, 257-262.	0.9	1
529	Nanoindentation investigation of solid-solution strengthening in III-V semiconductor alloys. International Journal of Materials Research, 2005, 96, 1237-1241.	0.8	3
530	High density InAlAs/GaAlAs quantum dots as an efficient enhanced Kerr material for transverse non-linear optics in microcavities. , 2005, , .		0
531	TEM determination of the local concentrations of substitutional and interstitial Mn and antisite defects in ferromagnetic GaMnAs. , 2005, , 147-150.		0
532	Effect of the p+-GaAs contact layer doping level on the gradual degradation of InGaAs/AlGaAs pump lasers. EPJ Applied Physics, 2004, 27, 465-468.	0.7	1
533	Long-range ordering of Ill–V semiconductor nanostructures by shallowly buried dislocation networks. Journal of Physics Condensed Matter, 2004, 16, 7941-7946.	1.8	3
534	GalnAs/GaAs quantum-well growth assisted by Sb surfactant: Toward 1.3â€,μm emission. Applied Physics Letters, 2004, 84, 3981-3983.	3.3	81
535	Buried dislocation networks designed to organize the growth of III-V semiconductor nanostructures. Physical Review B, 2004, 70, .	3.2	6
536	Indentation-induced crystallization and phase transformation of amorphous germanium. Journal of Applied Physics, 2004, 96, 1464-1468.	2.5	36
537	Determination of the Local Concentrations of Mn Interstitials and Antisite Defects inGaMnAs. Physical Review Letters, 2004, 93, 086107.	7.8	48
538	Absolute determination of the asymmetry of the in-plane deformation of GaAs (001). Journal of Applied Physics, 2004, 95, 3984-3987.	2.5	12
539	Polarity-induced changes in the nanoindentation response of GaAs. Journal of Materials Research, 2004, 19, 131-136.	2.6	18
540	Material and optical properties of GaAs grown on (001) Ge/Si pseudo-substrate. Materials Research Society Symposia Proceedings, 2004, 809, B2.4.1.	0.1	0

#	Article	IF	CITATIONS
541	Solid-solution strengthening in ordered InxGa1 â^ xP alloys. Philosophical Magazine Letters, 2004, 84, 373-381.	1.2	11
542	Further insight into the growth temperature influence of 1.3 μm GalnNAs/GaAs QWs on their properties. IEE Proceedings: Optoelectronics, 2004, 151, 279-283.	0.8	4
543	Growth of GaNxAs1â^'x atomic monolayers and their insertion in the vicinity of GaInAs quantum wells. IEE Proceedings: Optoelectronics, 2004, 151, 254-258.	0.8	6
544	Indentation punching through thin (011) InP. Journal of Materials Science, 2004, 39, 943-949.	3.7	16
545	Effects of GaNAsSb intermediate barriers on GalnNAsSb quantum well grown by molecular beam epitaxy. Journal of Crystal Growth, 2004, 263, 58-62.	1.5	5
546	TEM study of the indentation behaviour of thin Au film on GaAs. Thin Solid Films, 2004, 460, 150-155.	1.8	5
547	Photoluminescence probing of non-radiative channels in hydrogenated In(Ga)As/GaAs quantum dots. Journal of Crystal Growth, 2004, 264, 334-338.	1.5	3
548	Direct growth of GaAs-based structures on exactly (001)-oriented Ge/Si virtual substrates: reduction of the structural defect density and observation of electroluminescence at room temperature under CW electrical injection. Journal of Crystal Growth, 2004, 265, 53-59.	1.5	32
549	Structural studies of nano/micrometric semiconducting GalnP wires grown by MOCVD. Journal of Crystal Growth, 2004, 272, 198-203.	1.5	11
550	Morphology and composition of highly strained InGaAs and InGaAsN layers grown on GaAs substrate. Applied Physics Letters, 2004, 84, 203-205.	3.3	49
551	Vickers indentation of thin GaAs (001) samples. Philosophical Magazine, 2004, 84, 3281-3298.	1.6	10
552	Composition profiling of InAsâ^•GaAs quantum dots. Applied Physics Letters, 2004, 85, 3717-3719.	3.3	85
553	Thermal stability of ion-irradiated InGaAs with subpicosecond carrier lifetime. , 2004, , .		0
554	Polarity-induced changes in the nanoindentation response of GaAs. Journal of Materials Research, 2004, 19, 131-136.	2.6	2
555	Plasticity of misoriented (001) GaAs surface. Journal of Materials Science Letters, 2003, 22, 565-567.	0.5	4
556	Improvement of heteroepitaxial growth by the use of twist-bonded compliant substrate: Role of the surface plasticity. Journal of Electronic Materials, 2003, 32, 861-867.	2.2	2
557	Plastic deformation of III–V semiconductorsunder concentrated load. Progress in Crystal Growth and Characterization of Materials, 2003, 47, 1-43.	4.0	43
558	Structural properties of strained piezoelectric [111]A-oriented InGaAs/GaAs quantum well structures grown by MOVPE. Journal of Crystal Growth, 2003, 248, 359-363.	1.5	4

#	Article	IF	CITATIONS
559	N-enrichment at the GaAs1â^'xNx/GaAs(001) interface: microstructure and optical properties. Journal of Crystal Growth, 2003, 248, 441-445.	1.5	5
560	Comparison of GalnNAs/GaAs and GalnNAs/GaNAs/GaAs quantum wells emitting over 1.3μm wavelength. Journal of Crystal Growth, 2003, 251, 403-407.	1.5	16
561	Electromodulation of the interband and intraband absorption of Ge/Si self-assembled islands. Physica E: Low-Dimensional Systems and Nanostructures, 2003, 16, 450-454.	2.7	7
562	Silicon-on-insulator and SiGe waveguide photodetectors with Ge/Si self-assembled islands. Physica E: Low-Dimensional Systems and Nanostructures, 2003, 16, 523-527.	2.7	14
563	Characterization of piezoelectric and pyroelectric properties of MOVPE-grown strained (111)A InGaAs/GaAs QW structures by modulation spectroscopy. Physica Status Solidi A, 2003, 195, 260-264.	1.7	16
564	Phase separation and superlattice formation by spontaneous vertical composition modulation in GaAs1â^xNx/GaAs. Physica Status Solidi C: Current Topics in Solid State Physics, 2003, 0, 2749-2752.	0.8	0
565	Growth and optical characterizations of InAs quantum dots on InP substrate: towards a 1.5511/4 m quantum dot laser. Journal of Crystal Growth, 2003, 251, 230-235.	1.5	60
566	Indentation-induced deformations of GaAs(011) at a high temperature. Philosophical Magazine, 2003, 83, 1653-1673.	1.6	19
567	Control of nitrogen incorporation in Ga(In)NAs grown by metalorganic vapor phase epitaxy. Journal of Applied Physics, 2003, 94, 2752-2754.	2.5	10
568	Thermal stability of ion-irradiated InGaAs with (sub-) picosecond carrier lifetime. Applied Physics Letters, 2003, 82, 856-858.	3.3	28
569	Investigations on GalnNAsSb quinary alloy for 1.5 μm laser emission on GaAs. Applied Physics Letters, 2003, 83, 1298-1300.	3.3	50
570	Effects of annealing on structure of GaAs(001) nanoindentations. Philosophical Magazine Letters, 2003, 83, 149-158.	1.2	8
571	1.5â€[micro sign]m laser on GaAs with GalnNAsSb quinary quantum well. Electronics Letters, 2003, 39, 519.	1.0	33
572	Silicon–on–insulator waveguide photodetector with Ge/Si self-assembled islands. Journal of Applied Physics, 2002, 92, 1858-1861.	2.5	25
573	Microscopic structure and optical properties of GaAs1â~'xNx/GaAs(001) interface grown by metalorganic vapor phase epitaxy. Applied Physics Letters, 2002, 80, 2460-2462.	3.3	9
574	Origin of the bimodal distribution of low-pressure metal-organic-vapor-phase-epitaxy grown InGaAs/GaAs quantum dots. Journal of Applied Physics, 2002, 91, 3859-3863.	2.5	15
575	Transmission electron microscopy study of the InP/InGaAs and InGaAs/InP heterointerfaces grown by metalorganic vapor-phase epitaxy. Journal of Applied Physics, 2002, 92, 5749-5755.	2.5	47
576	Influence of the twist angle on the plasticity of the GaAs compliant substrates realized by wafer bonding. Journal of Physics Condensed Matter, 2002, 14, 12967-12974.	1.8	2

#	Article	IF	CITATIONS
577	Low-load deformation of InP under contact loading; comparison with GaAs. Philosophical Magazine A: Physics of Condensed Matter, Structure, Defects and Mechanical Properties, 2002, 82, 1953-1961.	0.6	5
578	Low-load deformation of InP under contact loading; comparison with GaAs. Philosophical Magazine A: Physics of Condensed Matter, Structure, Defects and Mechanical Properties, 2002, 82, 1953-1961.	0.6	17
579	Strength Enhancement of Compensated Strained InP/AIP Superlattice. Physica Status Solidi A, 2002, 189, 175-181.	1.7	2
580	Metal-organic vapor-phase epitaxy of defect-free InGaAs/GaAs quantum dots emitting around 1.3μm. Journal of Crystal Growth, 2002, 235, 89-94.	1.5	15
581	Subsurface deformations induced by a Vickers indenter in GaAs/AlGaAs superlattice. Journal of Materials Science Letters, 2002, 21, 401-404.	0.5	25
582	Bimodal distribution of Indium composition in arrays of low-pressure metalorganic-vapor-phase-epitaxy grown InGaAs/GaAs quantum dots. Applied Physics Letters, 2001, 79, 2157-2159.	3.3	25
583	Normal-incidence (001) second-harmonic generation in ordered Ga_05In_05P. Journal of the Optical Society of America B: Optical Physics, 2001, 18, 81.	2.1	6
584	Height dispersion control of InAs/InP quantum dots emitting at 1.55 μm. Applied Physics Letters, 2001, 78, 1751-1753.	3.3	164
585	Devitrification of fluorozirconate glasses: from nucleation to spinodal decomposition. Journal of Non-Crystalline Solids, 2001, 284, 85-90.	3.1	16
586	Plastic behaviour of an AlAs/GaAs superlattice with a short period. Philosophical Magazine Letters, 2001, 81, 223-231.	1.2	4
587	Plasticity of GaAs compliant substructures. Materials Science & Engineering A: Structural Materials: Properties, Microstructure and Processing, 2001, 309-310, 478-482.	5.6	1
588	New progresses in transparent rare-earth doped glass-ceramics. Optical Materials, 2001, 16, 255-267.	3.6	110
589	Influence of the thermal treatment on the optical and structural properties of 1.3 μm emitting LP-MOVPE grown InAs/GaAs quantum dots. Optical Materials, 2001, 17, 263-266.	3.6	5
590	Investigations on GaAsSbN/GaAs quantum wells for 1.3–1.55μm emission. Journal of Crystal Growth, 2001, 227-228, 553-557.	1.5	51
591	In-depth deformation of InP under a Vickers indentor. Journal of Materials Science, 2001, 36, 1343-1347.	3.7	14
592	Deformations of (011) GaAs under concentrated load. Journal of Materials Science Letters, 2001, 20, 1361-1364.	0.5	10
593	Non-linear solid solution strengthening of InGaAs alloy. Journal of Materials Science Letters, 2001, 20, 43-45.	0.5	11
594	Twist-bonded compliant substrates for III–V semiconductors heteroepitaxy. Applied Surface Science, 2001, 178, 134-139.	6.1	12

#	Article	IF	CITATIONS
595	Plasticity of GaAs(011) at room temperature under concentrated load. Philosophical Magazine Letters, 2001, 81, 527-535.	1.2	2
596	Onset of plasticity in a Σ = 5 GaAs compliant structure. Philosophical Magazine Letters, 2001, 81, 813-822.	1.2	2
597	Structural effects of the thermal treatment on a GaInNAs/GaAs superlattice. Applied Physics Letters, 2001, 79, 1795-1797.	3.3	28
598	Comparison of light- and heavy-ion-irradiated quantum-wells for use as ultrafast saturable absorbers. Applied Physics Letters, 2001, 79, 2722-2724.	3.3	34
599	Nanoindentation of GaAs compliant substrates. Philosophical Magazine A: Physics of Condensed Matter, Structure, Defects and Mechanical Properties, 2000, 80, 2899-2911.	0.6	24
600	Room-Temperature Plasticity of InAs. Physica Status Solidi A, 2000, 179, 153-158.	1.7	14
601	TEM study of the morphological and compositional instabilities of InGaAsP epitaxial structures. Journal of Crystal Growth, 2000, 221, 12-19.	1.5	15
602	GaAs/GaAs twist-bonding for compliant substrates: interface structure and epitaxial growth. Applied Surface Science, 2000, 164, 15-21.	6.1	15
603	Structural characterisation of transparent oxyfluoride glass-ceramics. Journal of Materials Science, 2000, 35, 4849-4856.	3.7	41
604	Structural characterisation of transparent oxyfluoride glass-ceramics. Journal of Materials Science, 2000, 35, 4849-4856.	3.7	27
605	Deformations induced by a Vickers indentor in InP at room temperature. EPJ Applied Physics, 2000, 12, 31-36.	0.7	16
606	All-optical discrimination at 1.5 [micro sign]m using an ultrafast saturable absorber vertical cavity device. Electronics Letters, 2000, 36, 1486.	1.0	19
607	Step-bunching instability in strained-layer superlattices grown on vicinal substrates. Applied Physics Letters, 2000, 76, 306-308.	3.3	9
608	Ultrafast saturable absorption at 1.55 μm in heavy-ion-irradiated quantum-well vertical cavity. Applied Physics Letters, 2000, 76, 1371-1373.	3.3	33
609	Strain and composition of capped Ge/Si self-assembled quantum dots grown by chemical vapor deposition. Applied Physics Letters, 2000, 77, 370-372.	3.3	35
610	Ge/Si self-assembled quantum dots grown on Si(001) in an industrial high-pressure chemical vapor deposition reactor. Journal of Applied Physics, 1999, 86, 1145-1148.	2.5	23
611	Transmission electron microscopy observations of low-load indents in GaAs. Philosophical Magazine Letters, 1999, 79, 805-812.	1.2	46
612	Morphological and Compositional Instabilities of Strained and Unstrained Alloy Layers. Materials Research Society Symposia Proceedings, 1999, 583, 315.	0.1	0

#	Article	IF	CITATIONS
613	High-quality InAs/GaAs quantum dots grown by low-pressure metalorganic vapor-phase epitaxy. Journal of Crystal Growth, 1998, 195, 524-529.	1.5	5
614	Planar selective regrowth of high resistivity semi-insulating InP(Fe) by LP-MOVPE for buried lasers using TBP. Journal of Crystal Growth, 1998, 195, 479-484.	1.5	4
615	Low-damage dry-etched grating on an MQW active layer and dislocation-free InP regrowth for 1.55-/spl mu/m complex-coupled DFB lasers fabrication. IEEE Photonics Technology Letters, 1998, 10, 1070-1072.	2.5	33
616	Optical studies of ultrashort-period GaAs/AlAs superlattices grown on (In,Ga)As pseudosubstrate. Physical Review B, 1998, 58, R7540-R7543.	3.2	1
617	Base metallization stability in InP/InGaAs heterojunction bipolar transistors and its influence on leakage currents. Journal of Vacuum Science & Technology an Official Journal of the American Vacuum Society B, Microelectronics Processing and Phenomena, 1997, 15, 854.	1.6	4
618	Anisotropic etching of InP with low sidewall and surface induced damage in inductively coupled plasma etching using SiCl4. Journal of Vacuum Science and Technology A: Vacuum, Surfaces and Films, 1997, 15, 626-632.	2.1	50
619	1.3 μm strain-compensated InAsP/InGaP electroabsorption modulator structure grown by atmospheric pressure metal–organic vapor epitaxy. Applied Physics Letters, 1997, 70, 96-98.	3.3	23
620	Metal organic vapor phase epitaxy growth of GaAsN on GaAs using dimethylhydrazine and tertiarybutylarsine. Applied Physics Letters, 1997, 70, 2861-2863.	3.3	97
621	Structure of the GaAs/InP interface obtained by direct wafer bonding optimised for surface emitting optical devices. Journal of Applied Physics, 1997, 82, 4892-4903.	2.5	61
622	Study of growth rate and composition variations in metalorganic vapour phase selective area epitaxy at atmospheric pressure and application to the growth of strained layer DBR lasers. Journal of Crystal Growth, 1997, 170, 639-644.	1.5	14
623	Controlled steam oxidation of AlInAs for microelectronics and optoelectronics applications. Journal of Electronic Materials, 1997, 26, L32-L35.	2.2	8
624	Transmission electron microscope observations of dislocations in heteroepitaxial layers of CdTe-(CdHg)Te on GaAs. Materials Science and Engineering B: Solid-State Materials for Advanced Technology, 1997, 45, 76-84.	3.5	3
625	Material Flow at the Surface of Indented Indium Phosphide. Physica Status Solidi A, 1997, 161, 415-427.	1.7	9
626	Submilliwatt optical bistability in wafer fused vertical cavity at 1.55-μm wavelength. IEEE Photonics Technology Letters, 1996, 8, 539-541.	2.5	12
627	Inhibition of thickness variations during growth of InAsP/InCaP and InAsP/InCaAsP multiquantum wells with high compensated strains. Applied Physics Letters, 1996, 69, 2279-2281.	3.3	23
628	Transmission Electron Microscopy Studies of Lattice-Mismatched Semiconductor Heterostructures Used for Integrated Optoelectronic Devices. Solid State Phenomena, 1996, 51-52, 131-142.	0.3	1
629	Kinematic versus dynamic approaches of xâ€ray diffraction simulation. Application to the characterization of InGaAs/InGaAlAs multiple quantum wells. Journal of Applied Physics, 1996, 79, 2332-2336.	2.5	6
630	Sidewall and surface induced damage comparison between reactive ion etching and inductive plasma etching of InP using a CH4/H2/O2 gas mixture. Journal of Vacuum Science and Technology A: Vacuum, Surfaces and Films, 1996, 14, 1056-1061.	2.1	36

#	Article	IF	CITATIONS
631	Gravure hélicon de l'InP en plasma HBr. Morphologie et caractérisation des défauts de surface. Journal De Physique III, 1995, 5, 467-481.	0.3	0
632	GaAs substrates for the MOVPE growth of (Hg,Cd)Te layers. Advanced Materials for Optics and Electronics, 1994, 3, 239-245.	0.4	6
633	Imperfections in Il–VI semiconductor layers epitaxially grown by organometallic chemical vapour deposition on GaAs. Journal of Crystal Growth, 1993, 129, 375-384.	1.5	10
634	Effect of the orientations and polarities of GaAs substrates CdTe buffer layer structural properties. Materials Science and Engineering B: Solid-State Materials for Advanced Technology, 1993, 16, 145-150.	3.5	20
635	Extended defects in II-VI semiconductor heteroepitaxial layers grown on GaAs substrates of various orientations. Physica Status Solidi A, 1993, 138, 437-443.	1.7	2
636	Interphases and mechanical properties in carbon fibres/Al matrix composites. European Physical Journal Special Topics, 1993, 03, C7-1693-C7-1698.	0.2	3
637	Misfit accommodation and dislocations in heteroepitaxial semiconductor layers: II-VI compounds on GaAs. Journal De Physique III, 1993, 3, 1189-1199.	0.3	9
638	Thermodynamic analysis of Zn-Cd-Te, Zn-Hg-Te and Cd-Hg-Te: phase separation in ZnxCd1â^'xTe and ZnxHg1â^'xTe. Journal of Crystal Growth, 1992, 117, 10-15.	1.5	60
639	Optical and structural properties of 1.3 $\hat{l}$ /4m emitting InAs/GaAs quantum dots grown by LP-MOVPE as a function of the re-growth temperature. , 0, , .		Ο
640	Wafer bonded all-optical switching devices. , 0, , .		0
641	Wet thermal oxidation of AlInAs and AlAsSb alloys lattice-matched to InP. , 0, , .		Ο
642	Cubic phase gallium nitride epitaxially formed on GaAs or GaInAs at low temperature with a NH3 DECR plasma. , 0, , .		0
643	Designing the relative impact of thickness/composition changes in selective area organometallic epitaxy for monolithic integration applications. , 0, , .		2
644	Low damage dry-etched grating on a MQW active layer and dislocation-free InP regrowth for 1.55 μm complex-coupled DFB lasers fabrication. , 0, , .		0
645	GaAsSbN: a material for 1.3-1.55 ν4m emission. , 0, , .		1
646	Ultrafast saturable absorber device with heavy-ion irradiated quantum wells for high bit-rate optical regeneration at 1.55 î¼m. , 0, , .		0
647	Detailed comparison of GalnNAs/GaAs and GalnNAs/GaNAs/GaAs quantum wells emitting near 1.3 μm wavelength. , 0, , .		Ο
648	MOVPE growth and characterization of long-wavelength emitting quantum dots based lasers at 300 K. , 0, , .		0

#	Article	IF	CITATIONS
649	Piezoelectric InGaAs/GaAs/AlGaAs quantum well lasers grown on (111)A GaAs by metalorganic vapor phase epitaxy. , 0, , .		0
650	Plasticity and Fracture of InP/Si Substructures. Materials Science Forum, 0, 783-786, 1628-1633.	0.3	0